

**Response to referee David Lazarus and an anonymous referee on
“Expansion and diversification of high-latitude radiolarian assemblages in
the late Eocene linked to a cooling event in the Southwest Pacific” by K. M.
Pascher et al.**

K. M. Pascher et al.

k.pascher@gns.cri.nz

We acknowledge the thorough review by David Lazarus and an anonymous referee that provided helpful comments on improving our manuscript. We will respond to each comment below (referees’ comments are shown in italics) and explain how we address each point.

Response to referee David Lazarus

Comment on prior studies: My first substantial criticism is that too little of this prior work is made visible to the reader of the current ms. Although several of these prior studies are cited, they are cited without providing any real information as to their content. Indeed, one might get the false impression from the Pascher ms that rather little has been known until now of southwestern Pacific plankton biogeographic evolution, or that the timing of ocean water mass origins is a new discovery, or that the sections used in this study have not been extensively examined already for radiolarian faunal characteristics. A brief but proper review of prior studies and the significance of the new ms results in the context of this prior work needs to be added to the introduction section of the paper.

Response: We agree with this comment and have revised the introduction chapter accordingly and included a review of previous work. Other parts of the introduction have been modified slightly.

Although Lazarus, Hollis and Apel (2008) used the same set of cores from the Southwest Pacific, and Hollis et al. (1997) and Crouch and Hollis (1996) analysed the radiolarian fauna of parts of DSDP sites 277, 280 and 281, respectively, we re-investigated the radiolarian fauna for all DSDP sites in this study, including new quantitative data and analysis, study of infill samples and review and application of revised identifications in light of more recent work, notably the study of ODP Site 1172 (Suzuki et al., 2009).

Revised text in the introduction:

The climate history of the early Paleogene has been established by geochemical proxies for temperature and paleontological data. The primary proxy record, stable oxygen isotope ($\delta^{18}\text{O}$) values of benthic foraminifera, shows a trend from an early Cenozoic greenhouse climate to an icehouse climate with the major shift in benthic $\delta^{18}\text{O}$ values of $\sim +1.5\text{‰}$ in the earliest Oligocene (~ 34 Ma) (Shackleton and Kennett, 1975; Diester-Haass et al., 1996; Zachos et al., 2001). After a prolonged period of maximum warmth during the Early Eocene Climatic Optimum (EECO) centred around 53–51 Ma, long-term cooling was interrupted by the Middle Eocene Climatic Optimum (MECO), a ~ 500 kyr period of warmth peaking ~ 40 Ma that has been linked to an increase in atmospheric $p\text{CO}_2$ (Bohaty and Zachos, 2003; Bohaty et al., 2009; Bijl et al., 2010). Lipid biomarker-based climate proxies (Liu et al., 2009; Bijl et al., 2010) suggest the Southwest Pacific sea surface temperatures

were tropical during the MECO (28°C) and continued to be warm throughout the late Eocene (24–26°C), cooling only slightly across the Eocene-Oligocene Transition (EOT, ~22°C). The generally warm conditions of the Eocene are consistent with fossil-based reconstructions of Southern Ocean circulation developed from high-latitude drill cores (Kennett, 1977; Nelson and Cooke, 2001; Kennett and Exon, 2004), in which subtropical waters are interpreted to have extended close to the Antarctic margin until the late Eocene. However, the latest generation of ocean circulation and climate modelling simulations fail to reproduce the degree of high-latitude warmth indicated for the Eocene by these new proxies (Hollis et al., 2012; Lunt et al., 2012). Even under hyper-greenhouse conditions, the models produce a cyclonic gyre that blocks subtropical waters from penetrating southward beyond 45°S (Huber and Sloan, 2001; Huber et al., 2004). High-latitude warmth also conflicts with increasing evidence for ephemeral Antarctic glaciation during the latest Eocene from both fossil and geochemical proxies (Lazarus and Caulet, 1993; Scher et al., 2014; Barron et al., 2015). Following the MECO event, benthic $\delta^{18}\text{O}$ values increased to their maximum Eocene values of ~2.3‰ at about 37.3 Ma during a short-lived cooling episode in the early late Eocene, referred to as the Priabonian Oxygen Isotope Maximum (PrOM) (Scher et al., 2014). Further climate oscillations are reported for the late Eocene (Vonhof et al., 2000; Pälike et al., 2001; Bohaty and Zachos, 2003; Villa et al., 2008; Westerhold et al., 2014) prior to the expansion of Antarctic ice that defines the EOT. A negative $\delta^{18}\text{O}$ excursion reported at ODP Sites 689 (Maud Rise), 738, 744, and 748 (Kerguelen Plateau) (Diester-Haass and Zahn, 1996; Bohaty and Zachos, 2003; Villa et al., 2008; Villa et al., 2014) has been interpreted to be a short-lived warming event in the late Eocene (~36.4 Ma).

Identifying the initial timing and establishment of a high-latitude fauna in the Southern Ocean helps to constrain the development of the Southern Ocean frontal systems and, in turn, heat transfer between low and high latitudes. Kennett (1978) provided the first summary on the biogeographic development of planktic biota in the circum-polar Southern Ocean throughout the Cenozoic. He inferred that the development of distinct polar plankton assemblages was related to the evolution of the Antarctic Circumpolar Current (ACC) and the Antarctic Polar Front (AAPF). This change was associated with the breakup of southern continents at the EOT and implicated as the main causal mechanisms for Antarctic glaciation. Subsequent deep-sea drilling campaigns resulted in more detailed studies about regional change in plankton and were integrated by Lazarus and Caulet (1993) into a set of circum-polar maps across specific time intervals. Moreover, these authors also carried out the first synthesis of radiolarian biogeography for the region and found a pattern of increasing endemism in the Southern Ocean across the EOT. Nelson and Cooke (2001) undertook a comprehensive review of previous work and presented an updated synthesis on the oceanic front development in the Southwest Pacific during the Cenozoic. According to these authors, a proto-Subtropical Front was established in the late Eocene (ca. 35 Ma) and an AAPF in the early Oligocene. A more detailed study of radiolarian biogeographic patterns and trends in the Southwest Pacific was done by Lazarus et al. (2008), who found increased endemism in the radiolarian fauna in the late Eocene (ca. 35 Ma). Further radiolarian studies from the Atlantic sector of the Southern Ocean were performed by Funakawa and Nishi (2008), who recorded the first expansion of an Antarctic assemblage significantly earlier (38.5 Ma). They identified several faunal turnover events associated with an increase or decrease in the Antarctic assemblage from the late middle Eocene to late Oligocene and linked these events to the northward or southward migration of the AAPF. Latest research suggests that the ACC was not developed until ~30 Ma, together with the establishment of an AAPF (Scher et al. 2015), when the Tasmanian gateway aligned with the westerly wind flow. From the middle to late Eocene, a westward Antarctic Slope Current is inferred to have flown across the gateway, driven by the polar easterlies (Bijl et al. 2013; Scher et al. 2015).

1 In this paper, we document variation in radiolarian assemblages and foraminiferal oxygen and carbon
2 stable isotopes from the middle Eocene-to-early Oligocene interval (~40 to 30 Ma) at DSDP Site 277
3 and relate these variations to radiolarian assemblage changes at DSDP Sites 280, 281, 283 and ODP
4 Site 1172. DSDP Site 277 provides a unique record of pelagic sedimentation in the Southwest Pacific
5 from the late Paleocene to Oligocene times and the first Eocene foraminiferal $\delta^{18}\text{O}$ record was
6 generated from this site (Shackleton and Kennett, 1975). Although Lazarus et al.'s (2008) study of
7 radiolarian assemblages included all above mentioned DSDP sites, this new work includes a more
8 thorough taxonomic review of the radiolarian assemblages at these sites and integrates the radiolarian
9 assemblage trends with new stable isotope data for Site 277. Our results help to identify the extent to
10 which tropical or warm-subtropical conditions prevailed during the middle and late Eocene, refine the
11 timing and nature of the development of a distinctive Southern Ocean radiolarian fauna and discuss
12 implications for the paleoceanography of the Southwest Pacific from the middle Eocene to early
13 Oligocene.

14 Comment on biogeographic assignments: *A second substantial criticism is the assignment of*
15 *individual radiolarian species to biogeographic categories, e.g. Antarctic, Tropical, etc. Paleogene*
16 *radiolarian biogeography unfortunately is not at all well known for most species, in contrast to the*
17 *more extensively studied, and far less diverse groups like foraminifera and calcareous nannofossils.*
18 *The early synthesis by Lazarus and Caulet was based primarily on the subjective but extensive*
19 *experience of the two authors (Lazarus for the Neogene, Caulet for the Paleogene) as there were at*
20 *the time no methods available to easily synthesise the scattered primary literature. Many tools are*
21 *now available which in principle allow a more rigorous, objective basis for biogeographic*
22 *interpretation, and I had hoped that this ms would provide this as a new, better foundation for current*
23 *and future research. The authors unfortunately do not provide any details as to how biogeographic*
24 *assignments were done for individual species, nor is this available from the SOM or the other papers*
25 *cited. This is a missed opportunity at the least. The ms needs to provide (in the SOM) a brief but*
26 *sufficient explanation as to why a given species is assigned to a biogeographic category. Funakawa*
27 *and Nishi's (2008) study gives a good example of how this can be presented - a set of sites with*
28 *radiolarian faunas from the time interval, marked by either presence-absence or relative abundance*
29 *symbols. The authors have available to them the materials (including the MRC collections used by*
30 *Funakawa and Nishi, one of which is housed at their institution) and if desired, access to global*
31 *published occurrence data, either via formal databases such as the NSB system or simple searches of*
32 *community shared pdf literature archives. Hopefully the authors have in fact done something similar*
33 *already and only need to provide the documentation.*

34 Response: We acknowledge this shortcoming in the SOM. In fact, we have followed the approach
35 recommended by the reviewer in most instances. However, we wish to emphasize that this current
36 work is part of an on-going project that will consist of a set of publications. The assignment of
37 biogeographic affinities in this manuscript is based on an intensive and critical taxonomic literature
38 review of radiolarian occurrences from the Southwest Pacific, Southern Ocean and other sites.
39 Because of the challenges in ensuring taxonomic names have been applied consistently, we have not
40 yet undertaken the same scrutiny of lower latitude records. However, we accept that we could have
41 made greater use of resources such as the NSB database to check the occurrences of relatively well-
42 known species.

43 Unfortunately, this database lacks many Paleogene radiolarians, and occurrence data are not always
44 robust and still need to be cross-checked with the DSDP/ODP reports. Also we observed that

presence/absence data are not always a reliable guide to biogeographic affinity. For instance, *Lithomelissa ehrenbergi* (Buetschli 1882) was described from Barbados, so one might consider this species as tropical or cosmopolitan. However, the species is far more abundant at high-latitude sites, and only rarely recorded at low-latitude sites. Moreover, Haeckel (1887) found recent *L. ehrenbergi* from deep-water samples at low latitudes. Therefore, we interpret this species as a cold-water indicator, commonly found in high-latitude samples and sometimes found in deep-water samples in low latitudes. We revised Table 1 and provide an additional table in the supplementary material with information on the biogeographic affinity of each species. Furthermore, we provide the paleolatitudes of all sites for certain age-ranges that we derived from www.paleolatitude.org (van Hinderbergen et al., 2015).

Comment on specific assignments (*L. minor*, *A. murrayanum*, *A. prolixum*): Nor are the biogeographic assignments given always plausible. For example, *Lithelius minor* is definitely cosmopolitan, although it does seem to be less common in tropical than temperate sections in the late Neogene. Also problematic are the two species (*A. murrayanum* and *A. prolixum*) which are the basis in the ms for inferring a tropical water conditions extending into polar regions in the Eocene. Both these species are reported in the literature in a wide variety of locations in the Paleogene: the Russian platform, Poland, Kamchatka, the northern Atlantic, Argentina and even well south of the Pascher study region, from the Kerguelen Plateau. Liu et al. (2011, *Palaeoworld*) explicitly challenge the claim that these species are tropical indicators.

Response: Although *L. minor* gr. seems to be more common in colder waters than in warmer, we agree that we cannot assign it to the high-latitude group. We assign this taxon to the cosmopolitan group, although we still want to single it out on revised Figures 6 and 7, as it is very abundant in the Southwest Pacific. The biogeographic affinities of *Amphicraspedum murrayanum* and *A. prolixum* group warrant some discussion. These taxa are widely reported in early and middle Eocene sediments but occur in greater abundance in the SW Pacific at times of global warmth (Hollis, 2006). The criticism raised by Liu et al. (2011) was based on the assumption that SW Pacific and North Atlantic Ocean conditions would have been similar in the Eocene. The assumption was said to be supported by an ocean circulation model (i.e. Huber et al. 2004), when in fact this model shows nothing of the sort (cf. Huber et al. 2003). The model indicates that oceanic conditions for the North Atlantic and the Southwest Pacific are substantially different: the North Atlantic is bathed in warm currents of ~25°C moving northwards (Fig. 1 below), while the SW Pacific is influenced by a strong cyclonic gyre preventing warm waters from penetrating southwards, except during times of extreme global warmth (see Fig. 2 and Hollis et al. 2012). Thus, the occurrence of warm water indicators throughout the Paleocene-Eocene interval in the mid-latitude North Atlantic is consistent with both the GCM results and our interpretation of influxes of *Amphicraspedum* as being indicative of warming. The significance of occurrences of this genus in other high-latitude regions still needs to be assessed with reference to its abundance and the timing of its occurrence.

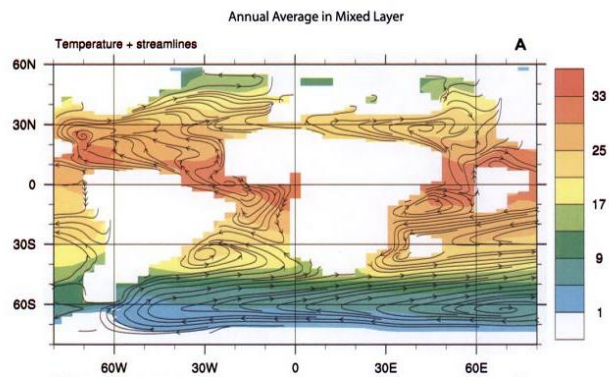


Fig. 1 from Huber et al. (2003) showing annual average temperatures in mixed layer.

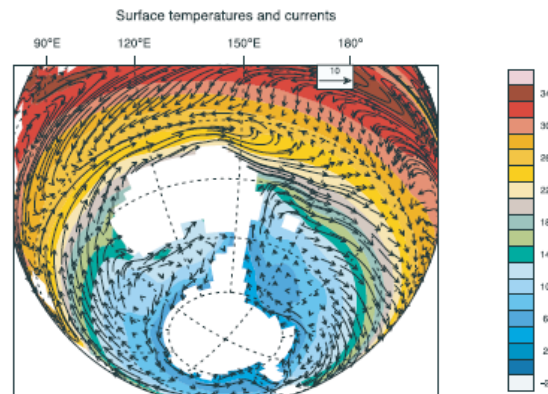


Fig. 2 from Huber et al. (2004), modelled sea surface temperatures and velocity results.

In order to gain more insight into how assemblages at Site 277 changed in response to short-lived warming events, we have examined 5 additional samples (core 23R-1, 100cm, 23R-2, 22cm, 23R-2, 100cm, 23R-3, 20cm and 23R-3, 100cm) that lie within a late Eocene warming event based on the stable isotope record. We included these samples in revised versions of Figures 4, 6, 7 and 8. Within this interval, high-latitude taxa drop, *Lithomelissa* spp. and *Larcopyle* spp. are rare or absent. At the same time, cosmopolitan taxa increase (e.g. *Lychnocanium* spp.) and *Thyrsocyrtis pinguisicoides*, that we now assign to the low-latitude group, is abundant. Interestingly, Artostrobiidae are completely absent, but are very abundant directly before and after this event.

Comment on data analysis and biogeographic affinities: Another issue is the data analysis. I do not see anything in it that, if done differently is likely to completely change the interpretations, but nonetheless there are some weaknesses that could be improved, and which might well also improve the clarity of the results. The most important here is the use of percent values for biogeographic categories that include the most common category of 'unknown'. This makes the patterns, e.g. the

time series changes particularly sensitive to the amount of unknowns. This is problematic because the percent unknown is partially a function of preservation/ abundance in the sediment, as can be seen in Figure 6 - taxic richness correlates with % unknown throughout the lower half of the main data series in Site 277, and taxic richness in this interval is certainly a function of abundance since the sample count values are very low (see the spread sheet in the SOM - a plot of species richness vs total count [attached - not fully kosher as it is not one sample, but at least all from one site] gives a typical sampling curve where true richness values are only seen for counts in excess of ca 2,000 specimens). The specific mechanism linking this to % unknown can only be guessed at but probably reflects poorer preservation increasing the number of individuals not identifiable to species level. I suggest recalculating the biogeographic affinities to % of individuals that have been assigned to a biogeographic category only. I suspect that the resulting plots will show the trends claimed in the paper even better than the current figures do.

Response: We removed the “Unknown” group from Figs. 6 and 7, showing biogeographic affinity assignment only. As suggested by the reviewer, the observed patterns are now more clearly identifiable. Furthermore, we changed the colour for *L. minor* gr. to green (cosmopolitan group). We still think it is important to single this group out as it makes a large percentage of the assemblages. Since Figs. 6+7 now show only the species assigned to a biogeographic affinity group, we have recalculated Table 2 accordingly with the % of high-latitude taxa derived from the number of taxa assigned to one of the three groups (high-latitude, cosmopolitan, low-latitude).

Comment on diversity measurements: Also, given the fully typical dependence of raw species richness on sample size, if the authors wish to mention diversity in any other sense than as a synonym for abundance (which is the current state of the ms) they should use some sort of subsampling procedure, as is long standard in other areas of biology-paleontology. Simple rarefaction might be adequate in this material. I would only include species level identifications in this.

Response: We recognize that the lower the counts, the less reliable diversity measurements are. Indeed, the low abundance counts at Site 277 correlate with preservation, resulting in diversity measures and taxic richness being overall underestimated. Following the reviewer’s recommendation, we applied an ‘Individual rarefaction’ analysis for taxic richness by using the software package “PAST”, which allows to compare taxonomical diversity in samples of different size. We added the derived taxic richness for Site 277 in Figure 4, and used the Fisher alpha diversity measure in Figure 7 for all sites instead of taxic richness.

For site 277 we show the calculated taxic richness for 100, 200, 300 and 500 counts, respectively (Figure 4 revised). Our study shows that counts of at least 300 specimens are required to get a reliable measure of diversity and richness. Thus, diversity measures are considered unreliable where counts are < 300 and diversity is underestimated. However, a sample size of 100 specimens shows the observed trends as well. It was not always possible to achieve this minimum value in our sparse samples (9 samples yielded less than 100 specimens). We therefore removed all samples that have less than 100 specimens from Figures 6 and 7 for Site 277.

Although not commented upon by the reviewer, we also calculated the range-through taxic richness after subsampling for Site 277 with R (www.r-project.org) (Figure 4 revised) to see if the diversity drop between 230–290 mbsf is a preservational artefact or a real temporary absence. We have chosen sample sizes of 100 and 300, respectively, which show a similar pattern (both with a subsampling of 1000). According to this analysis, taxic richness is higher as observed from samples of Core-26 to Core 32 (~235–292 mbsf). Chert nodules are present from 246 mbsf downcore, so the absence of species in the interval between 246–350 mbsf seems to be an artefact of diagenesis. However, during the MECO, taxic richness increases. The results also show the increase in taxa related to the ProM event around ~225 mbsf, but do not show the observed decrease of taxa during the late Eocene warming event, but instead a slight increase. In conclusion, derived range-through taxic richness can be a helpful tool in determining the presence/absence of taxa due to diagenesis or real temporary

1 absence. But to distinguish between these two scenarios, it is essential to analyse the nature of the
2 sediment (e.g. chert nodules) as well as the nature of faunal assemblages (e.g. presence/absence of
3 high-latitude/low-latitude taxa).

4
5 Comment on ODP 1172 data: *There is an issue with the Site 1172 data, which forms a significant part*
6 *of the analysis. Unlike the other data this is not in the SOM or cited publications - the 2009 Suzuki*
7 *paper is just a taxonomic survey. It would be better to have this data in the SOM, and Suzuki added as*
8 *a junior author for the ms.*

9
10 Response: The census counts for Site 1172 formed part of a Master's project by Kentaro Chiba and
11 was provided to us by Noritoshi Suzuki. At the time of submitting this article, we were not sure of Mr
12 Chiba's plans for publication. After further discussion with Dr Suzuki, we have very willingly agreed
13 to add Suzuki and Chiba as co-authors to this paper. The census data are now provided in the SOM.

14
15 Comment on isotopes: *Lastly, a comment on the isotopes. I am not very convinced by the correlations*
16 *shown - the only feature of the new data that seems clear is the oxygen isotope shift equivalent to the*
17 *E-O boundary. It might be better to show each Site's age models (in the SOM) and plot the isotope*
18 *data for both 277 and the reference site 689 vs age, adding correlation lines based on biostrat events.*
19 *This might make the claimed correlations of the very gappy data in 277 to 689 more plausible.*

20
21 Response: We agree that Figure 2 needs some improvements in correlation (revised Figure 2). We
22 enlarged the isotope plot for Site 689 so the three events (EOT, PrOM and MECO) are approximately
23 on the same level to Site 277, which makes it easier to compare. We have chosen not to develop an
24 age model for Site 277 because there are significant uncertainties relating to sampling gaps and over
25 the age of some bioevents. However, we recognise the benefit of showing how key bioevents support
26 the correlation of isotope records between Sites 277 and 689. The isotope record at Site 689 and the
27 bioevents at Site 277 are both calibrated to the 2012 geological timescale (Gradstein et al., 2012;
28 Raine et al., 2015). We recognized that the MECO is a very thick interval at Site 277. However, this is
29 due to the poor core recovery and especially the core gaps of about 10m between cores 32 and 33, 33
30 and 34, and 34 and 35, respectively. The onset of the MECO is clearly identifiable, however due to
31 the incomplete record, the top of the event is uncertain. The same holds for the PrOM event, the base
32 is clearly identifiable; however the top of the event is uncertain due to the incomplete record.

33 **Further comments on the manuscript by David Lazarus**

34
35
36 Comment p. 2981: *to point (i) previously documented in Lazarus et al 2008. OK to question this and*
37 *thus wish to test but please explain reasons for doubt.* (text in ms: We use these data to test if i) a
38 distinct Southern Ocean fauna was established prior to the major shift in oxygen isotopes in the
39 earliest Oligocene)

40
41 Response: We don't question the general results of Lazarus et al. (2008). However, we wanted to see
42 if the timing of the establishment of a Southern Ocean fauna in the SW Pacific could be refined.
43 Indeed our results show that the turnover is not as sudden as that indicated by Lazarus et al. (2008), as
44 high-latitude taxa increase from the middle Eocene. However, the major increase happens in the late
45 Eocene and we are able to tie this change to the PrOM event. The major outcome of our work is the
re-analysis of the Southwest Pacific sites and the integration with stable isotopes.

46 We revised the final part of the introduction to the following:

47 Although Lazarus et al.'s (2008) study of radiolarian assemblages included all above mentioned
48 DSDP sites, this new work includes a more thorough taxonomic review of the radiolarian assemblages
49 at these sites and integrates the radiolarian assemblage trends with new stable isotope data for Site

277. Our results help to identify the extent to which tropical or warm-subtropical conditions prevailed during the middle and late Eocene, refine the timing and nature of the development of a distinctive Southern Ocean radiolarian fauna and discuss implications for the paleoceanography of the Southwest Pacific from the middle Eocene to early Oligocene.

Comment: *P. 2981: please comment on rotary disturbance*

Response: We have analysed the scientific report of DSDP Leg 29 on core disturbance, and include this information in the supplementary data file for each site and sample. We categorized disturbance as 'intact' (I), 'blocks' (B), 'disturbed' (D) with occurring 'slurry' (s) or 'breccia' (b) features and added that information in the SOM. However, in addition to the large gaps between cores 32–35, the degree of disturbance is very variable throughout a core on cm-scale (according to core photographs of DSDP Site 277 report). Cores are mainly intact and coherent between core 15 and 25, the sediment changing to 'blocks' in the remaining cores, with breccia or slurry deformation.

Comment: *P. 2984 Need to clarify depth habitat for these taxa - which is benthic, planktic.*

Response: We updated the manuscript with the following:

At the University of California Santa Cruz (UCSC) and the University of Southampton (UoS), stable oxygen ($\delta^{18}\text{O}$) and carbon ($\delta^{13}\text{C}$) isotope ratios were determined for bulk carbonate, benthic foraminifera (*Cibicidoides* spp.), and the planktic foraminifera *Subbotina* spp. (thermocline) from 332.62–159.88 mbsf and *Globigerinatheka* index (mixed layer) from 332.62–188.58 mbsf (its last occurrence). In total, a set of 157 samples spanning the middle Eocene-to-lower Oligocene interval of DSDP Hole 277 was measured. Stable isotope analyses at UCSC were performed on a VG Prism dual-inlet mass spectrometer coupled to carousel preparation device with common acid bath maintained at 90°C. Analyses at the UoS were performed on a Europa GEO 20-20 dual-inlet mass spectrometer with CAPS preparation oven maintained at 70°C. All values are reported relative to the Vienna Pee Dee Belemnite (VPDB) standard. In both labs, analytical precision based on replicate analyses of in-house marble standards and NBS-19 averaged $\sim 0.05\text{‰}$ (1σ) for $\delta^{13}\text{C}$ and $\sim 0.08\text{‰}$ (1σ) for $\delta^{18}\text{O}$.

Comment: *P. 2985: more detail on preservation helpful as Paleogene diagenetic biases are common even in superficially well preserved specimens.*

Response: There is no reason to suspect a large diagenetic bias as a normal gradient exists between benthic, subsurface and surface dwelling planktic isotopic values (revised Figure 3). However, as benthic values are more reliable than planktics, we focused our interpretation on benthic isotopes.

Comment: *P.2995: This appears to have been pulled out of thin air. Please explain how a quantitative temperature estimate is made from what we know of Paleogene radiolarian temperature correlations.*

Response: The important message is that the temperatures were not tropical in the middle to late Eocene in the SW Pacific at the investigated sites, because low-latitude radiolarians are only present in rare numbers, and typical taxa encountered in low-latitude sites (*Podocyrthis*, *Thyrsocyrtis*) are missing. Based on the stable isotopes and the radiolarian fauna, we are able to identify the late Eocene warming event $\sim 36.4\text{Ma}$ (Bohaty and Zachos, 2003), with a common presence of *Thyrsocyrtis pinguisicoides*, which we consider to be a warm-water indicator. The absence of other low-latitude taxa suggests modest warming, possibly to subtropical conditions.

We have revised the text to the following:

The persistence of high-latitude taxa and the variety of cosmopolitan species at both sites suggests a warm-temperate climate (15–20°C; Nelson and Cooke, 2001), in contrast to geochemical proxies suggesting a tropical climate (> 25°C) for the MECO at Site 1172 (Bijl et al., 2010) and ~27°C for the late Eocene at Site 277 (Liu et al., 2009). These temperature estimates were derived from organic proxies (TEX₈₆ and U^K₃₇) and the sea surface temperature estimates might be biased towards summer temperatures (Liu et al., 2009; Hollis et al., 2012). The relatively low abundance of Tropical radiolarian taxa within the PETM and early Eocene climatic optimum in the Southwest Pacific has been previously noted by Hollis (2006; Hollis et al., 2014).

Comment: P. 2997: The ca 20 m interval is also where rad abundance is extremely low, which is most likely indeed a preservation artifact, if not a diagenetic one.

Response: We replaced “artefact of preservation” on p. 2997, line 1 with “artefact of diagenesis”.

Comment: P. 3018: site 283 seems plotted at wrong age map.

Response: We have changed the maps, due to additional comments by referee two. Please see below (revised Figure 8).

Response to anonymous referee

Comment: The authors mention, almost in passing, that their faunal and geochemical results are in conflict with the geochemical records of Bijl et al., 2010 and Liu et al., 2009. The authors should at least attempt an explanation of why this discrepancy exists.

Response: We agree with this comment. We will expand this section in the manuscript. We can address this issue now in more detail as we have obtained 5 samples within the late Eocene warming interval.

Comment: My biggest issue with the manuscript is the tectonic reconstruction and inferred circulation patterns shown in Fig. 8.

Response: We apologize for not having given enough explanation and details about the tectonic reconstructions used in the previous manuscript. We now include information from a recent publication by van Hinsbergen et al. (2015) and are now using the following reconstructions:

Tectonic reconstructions of the Australia-Antarctica-Pacific plate circuit were undertaken in GPlates (Boyden et al., 2011) using finite poles of rotation for the relative motions between Australia-East Antarctica from Cande and Stock (2004) (0-38.13 Ma); East Antarctica-West Antarctica from Granot et al. (2013) (30.94-40.13 Ma); and West Antarctica-Pacific from Croon et al. (2008) (0-47.54 Ma). Relative motions of the Australia-Antarctica-Pacific plate circuit were tied to the Australian paleomagnetic apparent polar wander path of Torsvik et al. (2012) to provide an estimate of paleolatitude appropriate for paleoclimate studies (van Hinsbergen et al., 2015). The 2000 m isobath from the GEBCO bathymetric grid was used to approximate continental boundaries. The continental/oceanic boundaries of Bird (2003) are also shown (dashed lines in Figure 1 and 8) for reference for regions where extension has significantly thinned continental crust. DSDP/ODP sites have been assigned to the appropriate plate for reconstruction.

The overlap of the North and South Islands of New Zealand is a consequence of the finite poles of rotation from the Adare Trough of Granot et al. (2013) describing the motion of East and West

Antarctica between 40 and 30 Ma. These new poles result in a poor fit (significant overlap) of continental crust between the two islands that is not supported by geological data. These issues were not addressed in a recent publication by Matthews et al. (2015). The discrepancy between geological and paleomagnetic data could be reconciled with the use of seafloor spreading data from the Emerald basin (e.g. Keller, 2003), which describes Australia-Pacific relative motions (Sutherland, 1995) between 40 to 30 Ma, and the Adare Trough. No published reconciliation is presently known to the authors.

***Comment:** Also the authors need to clarify what they mean in reference to the Tasmanian Gateway being fully open (example is line 15 page 24). Fully open meaning to deep waters? The geophysics of the COB and tectonic reconstructions allow for fairly explicit ages for a deep connection. A deep connection was established 33.5 +/- 1.5 Ma. I would also like the authors to consider that water mass reconstructions of Scher et al., 2015 support the hypothesis by Bijl et al., 2013 that the first current to flow through the gateway flowed westward (from Pacific to Indian), probably under the influence of the polar easterlies, as the gateway was in a more southerly position. I do not think that the flow regime described by Scher et al., 2015 is inconsistent with the faunal and geochemical results presented here, though the authors should consider this. The above flow regime persisted until 30-29 Ma, when the northern margin of the gateway appears to have crossed into the westerlies. The arrow currently drawn through the gateway in the reconstructions in Fig. 8 is not consistent with the recent water mass reconstructions (Scher et al., 2015). I also think that the label ACC should be removed from panel D. The large scale homogenization of water mass tracers throughout the Southern Ocean, pointing to establishment of the ACC, does not occur until after 29 Ma.*

Response: We have updated Figure 8 accordingly. We will revise the text in the manuscript.

We have revised Fig. 8B by showing the early late Eocene interval (~38–37 Ma), that includes the PrOM event for Site 277 and adding a Subtropical Front (STF) across the Tasman Sea, which seemed to have been a high-productive upwelling region. According to Nelson and Cooke (2001), the STF was the first front to be established. We have also added the westward flowing Antarctic Slope Current (ASC) according to Bijl et al. (2013) and Scher et al. (2015).

Furthermore, we have added Figure 8C in order to show the late Eocene warming event (~36 Ma), which is evident at Sites 283 and 277 by an influx of low-latitude taxa. We interpret this as a short southward shift of the East Australian Current (EAC) and a weakening of the Ross gyre. However, the STF shifted southwards along the Campbell Plateau and Site 277 did not experience high-productivity.

Figure 8D shows the latest Eocene-earliest Oligocene interval (~35–32 Ma), with widespread non-deposition across the Tasman region and a highly productive area at Site 277. A strong Ross gyre created upwelling and a northward shift of the STF on the Campbell Plateau. In the south, Site 280 has an earliest Oligocene record only, showing a high-productivity diatom-rich endemic radiolarian assemblage.

Finally the early Oligocene map 8E shows a distinctly high-latitude assemblage for Sites 1172 and 277. We infer from Site 277, that this condition is similar to today's (oligotrophic, cold-water environment on the Campbell Plateau), which resulted in a decrease in radiolarian abundance. Both Sites 1172 and 277 contain the dominant high-latitude species *Axoprunum irregularis*. We interpret this scenario to signify the start of the Antarctic Circumpolar Current (ACC) around ~30 Ma, adapted from Carter et al. (2004), with the Tasmanian Gateway situated at about 60°S.

References

- Bird, P.: An updated digital model of plate boundaries, *Geochemistry, Geophysics, Geosystems*, 4, 2003.
- Bohaty, S. M., and Zachos, J. C.: Significant Southern Ocean warming event in the late middle Eocene, *Geology*, 31, 1017-1020, 2003.
- Boyden, J. A., Müller, R. D., Gurnis, M., Torsvik, T. H., Clark, J. A., Turner, M., Ivey-Law, H., Watson, R. J., and Cannon, J. S.: Next-generation plate-tectonic reconstructions using GPlates, *Geoinformatics: cyberinfrastructure for the solid earth sciences*, 95-114, 2011.
- Cande, S. C., and Stock, J. M.: Pacific—Antarctic—Australia motion and the formation of the Macquarie Plate, *Geophysical Journal International*, 157, 399-414, 2004.
- Carter, L., Carter, R., and McCave, I.: Evolution of the sedimentary system beneath the deep Pacific inflow off eastern New Zealand, *Marine Geology*, 205, 9-27, 2004.
- Croon, M. B., Cande, S. C., and Stock, J. M.: Revised Pacific-Antarctic plate motions and geophysics of the Menard Fracture Zone, *Geochemistry, Geophysics, Geosystems*, 9, 2008.
- Gradstein, F., Ogg, J., Schmitz, M., and Ogg, G.: *The geologic time scale 2012*, vol. 2, Elsevier New York, 2012.
- Granot, R., Cande, S., Stock, J., and Damaske, D.: Revised Eocene-Oligocene kinematics for the West Antarctic rift system, *Geophysical Research Letters*, 40, 279-284, 2013.
- Hollis, C. J.: Radiolarian faunal turnover through the Paleocene-eocene transition, Mead Stream, New Zealand, in: *Radiolaria*, Springer, 79-99, 2006.
- Huber, M., Sloan, L. C., and Shellito, C.: Early Paleogene oceans and climate: A fully coupled modeling approach using the NCAR CCSM, *Geological Society of America Special Papers*, 369, 25-47, 2003.
- Huber, M., Brinkhuis, H., Stickley, C. E., Döös, K., Sluijs, A., Warnaar, J., Schellenberg, S. A., and Williams, G. L.: Eocene circulation of the Southern Ocean: Was Antarctica kept warm by subtropical waters?, *Paleoceanography*, 19, PA4026, doi:10.1029/2004PA001014, 2004.
- Keller, W.R., 2003. Cenozoic plate tectonic reconstructions and plate boundary processes in the Southwest Pacific. Unpub. PhD Thesis: California Institute of Technology. Pasadena.
- Liu, J., Aitchison, J. C., and Ali, J. R.: Upper Paleocene radiolarians from DSDP Sites 549 and 550, Goban Spur, NE Atlantic, *Palaeoworld*, 20, 218-231, 2011.
- Matthews, K. J., Williams, S. E., Whittaker, J. M., Müller, R. D., Seton, M., and Clarke, G. L.: Geologic and kinematic constraints on Late Cretaceous to mid Eocene plate boundaries in the southwest Pacific, *Earth-Science Reviews*, 140, 72-107, 2015.
- Nelson, C. S., and Cooke, P. J.: History of oceanic front development in the New Zealand sector of the Southern Ocean during the Cenozoic—a synthesis, *New. Zeal. J. Geol. Geop.*, 44, 535-553, 2001.

1 Raine, J. I., Beu, A. G., Boyes, A. F., Campbell, H. J., Cooper, R. A., Crampton, J. S., Crundwell, M.
2 P., Hollis, C. J., and Morgans, H. E. G.: Revised calibration of the New Zealand Geological
3 Timescale : NZGT2015/1, Lower Hutt, N.Z.: GNS Science. GNS Science report 2012/39. 53 p, 2015.
4 Sutherland, R.: The Australia-Pacific boundary and Cenozoic plate motions in the SW Pacific: Some
5 constraints from Geosat data, *Tectonics*, 14, 819-831, 1995.
6 Torsvik, T. H., Van der Voo, R., Preeden, U., Mac Niocaill, C., Steinberger, B., Doubrovine, P. V.,
7 van Hinsbergen, D. J., Domeier, M., Gaina, C., and Tohver, E.: Phanerozoic polar wander,
8 palaeogeography and dynamics, *Earth-Science Reviews*, 114, 325-368, 2012.
9 van Hinsbergen, D. J., de Groot, L. V., van Schaik, S. J., Spakman, W., Bijl, P. K., Sluijs, A.,
10 Langereis, C. G., and Brinkhuis, H.: A Paleolatitude Calculator for Paleoclimate Studies, *PloS one*,
11 10, e0126946, 2015.
12
13 Revised manuscript with track changes below.
14

Expansion and diversification of high-latitude radiolarian assemblages in the late Eocene linked to a cooling event in the Southwest Pacific

K. M. Pascher^{1,2}, C. J. Hollis¹, S. M. Bohaty³, G. Cortese¹, ~~and R. M. McKay²~~, H. Seebeck¹, N. Suzuki⁴ and K. Chiba⁴

[1] GNS Science, P O Box 30368, Lower Hutt 5040, New Zealand

[2] Victoria University Wellington, Antarctic Research Centre, P O Box 600, Wellington 6140, New Zealand

[3] Ocean and Earth Science, University of Southampton, National Oceanography Centre Southampton, ~~University of Southampton Waterfront Campus~~, European Way, Southampton SO14 3ZH, United Kingdom

[4] Institute of Geology and Paleontology, Graduate School of Science, Tohoku University, Sendai City, 980-8578, Japan

Correspondence to: K. M. Pascher (k.pascher@gns.cri.nz)

Abstract

~~The Eocene was characterised by “greenhouse” climate conditions that were gradually terminated by a long-term cooling trend through the from middle to and late Eocene. This long-term trend was determined-punctuated by several large-scale climate perturbations that culminated in a shift to “ice-house” climates at the Eocene-Oligocene T_i transition. Geochemical and micropaleontological proxies suggest that tropical to subtropical sea-surface temperatures persisted into the late Eocene in the high-latitude Southwest Pacific Ocean. Here, w~~We present radiolarian microfossil assemblage and foraminiferal oxygen and carbon stable isotope data from Deep Sea Drilling Project (DSDP) ~~Sites-sites~~ 277, 280, 281, ~~and 283 and Ocean Drilling Project (ODP) Site 1172 from the middle Eocene to early Oligocene (~40–33 Ma)~~ to identify significant oceanographic changes in the Southwest Pacific ~~across-through this major climate transition (~40–30 Ma) in Earth’s climate history.~~ We find that T_i the Middle Eocene Climatic Optimum at ~40 Ma, which is truncated but

characterised-identified by a negative shift in foraminiferal $\delta^{18}\text{O}$ oxygen isotope values at Site 277, is associated with ~~and a radiolarian assemblage consisting of about 5% of low-latitude taxa *Amphiceraspedum prolixum* group and *Amphymenium murrayanuma*~~ small increase in radiolarian taxa with low-latitude affinities (5% of total fauna). In the early late Eocene at ~37 Ma, a positive oxygen isotope shift at Site 277 ~~is can be~~ correlated to the Priabonian Oxygen Isotope Maximum (PrOM) ~~event—a short-lived cooling event recognized throughout the Southern Ocean~~. Radiolarian abundance, diversity, and preservation increase ~~during the middle-of-within~~ this cooling event at Site 277 at the same time as diatoms abundance. A negative $\delta^{18}\text{O}$ excursion above the PrOM is correlated with a late Eocene warming event (~36.4 Ma). Radiolarian abundance and diversity decline within this event and taxa with low-latitude affinities reappear. Apart from this short-lived warming event, ~~the~~ the PrOM and latest Eocene radiolarian assemblages are characterised by abundant high-latitude taxa. ~~These~~ ~~High-latitude taxa are also abundant-increase in abundance-~~ during the late Eocene and early Oligocene (~38–30 Ma) at DSDP ~~S~~ sites 280, 281, ~~-and-283~~ and 1172 and are associated with very high diatom abundance. We therefore infer a northward expansion of high-latitude radiolarian taxa onto the Campbell Plateau ~~towards the end of the late~~ in the latest Eocene. In the early Oligocene (~~~33 Ma~~) there is an overall decrease in radiolarian abundance and diversity at Site 277, and diatoms are ~~absent~~ scarce. These data indicate that, once the Antarctic Circumpolar Current was established ~~Tasman Gateway was fully open~~ in the early Oligocene (~30 Ma), a frontal system similar to the present day ~~was established~~ developed, with nutrient-depleted ~~subantarctic~~ Subantarctic waters bathing the area around DSDP Site 277, resulting in a more ~~oligotrophic-restricted~~ siliceous plankton assemblage.

1 Introduction

The long-term evolution of climate ~~history-of-through~~ the early ~~to-mid~~ Paleogene (56–34 Ma) has been established ~~by-from~~ geochemical proxies ~~for temperature, loosely linked to and~~ paleontological data. The primary proxy record, stable oxygen isotope ($\delta^{18}\text{O}$ -) values of benthic foraminifera, shows a trend from an early Cenozoic greenhouse climate to an icehouse climate with ~~an abrupt positive-the major~~ shift in benthic $\delta^{18}\text{O}$ values of ~~~+~1.2-~~ 1.5‰ in the earliest Oligocene (~34 Ma) (Shackleton and Kennett, 1975; Diester-Haass et al., 1996; Zachos et al., 2001). After a prolonged period of maximum warmth during the Early Eocene Climatic Optimum (~~EECO~~) centred around 53–51 Ma, long-term cooling was

interrupted by the Middle Eocene Climatic Optimum (MECO), a ~500 kyr period of warmth peaking ~40 Ma that has been linked to an increase in atmospheric pCO₂ (Bohaty and Zachos, 2003; Bohaty et al., 2009; Bijl et al., 2010). ~~Organic-Lipid~~ biomarker-based climate proxies ~~(Liu et al., 2009; Bijl et al., 2010)~~ suggest the Southwest Pacific sea surface temperatures were tropical during the MECO (28°C) and continued to be warm throughout the late Eocene (24–26°C), cooling only slightly across the Eocene-Oligocene transition (EOT, ~22°C-) ~~(Liu et al., 2009; Bijl et al., 2010).~~

The warm conditions of the Eocene indicated by geochemical proxies are generally consistent with fossil-based reconstructions of Southern Ocean circulation developed from high-latitude drill cores (Kennett, 1977; Nelson and Cooke, 2001; Kennett and Exon, 2004; Houben et al., 2013), in which subtropical waters are interpreted to have extended close to the Antarctic margin until the late Eocene. However, the latest generation of ocean circulation and climate modelling simulations fail to reproduce the degree of high-latitude warmth indicated for the Eocene by these new proxies (Hollis et al., 2012; Lunt et al., 2012). Even under hyper-greenhouse conditions, the models produce a cyclonic gyre that blocks subtropical waters from penetrating southward beyond 45°S (Huber and Sloan, 2001; Huber et al., 2004). High-latitude warmth also conflicts with increasing evidence for ephemeral Antarctic glaciation during the latest Eocene from both fossil and geochemical proxies (Lazarus and Caulet, 1993; Scher et al., 2014; Barron et al., 2015). Following the MECO event, benthic $\delta^{18}\text{O}$ values increased to their maximum Eocene values of ~2.3‰ at about 37.3 Ma during a short-lived cooling episode in the early late Eocene, ~~designated-referred to~~ as the Priabonian Oxygen Isotope Maximum (PrOM) ~~event~~ (Scher et al., 2014). Further climate oscillations are reported for the late Eocene (Vanhof et al., 2000; Pälike et al., 2001; Bohaty and Zachos, 2003; Villa et al., 2008; Westerhold et al., 2014) prior to the expansion of Antarctic ice that defines the EOT. A negative $\delta^{18}\text{O}$ excursion reported at ODP sites 689 (Maud Rise), 738, 744, and 748 (Kerguelen Plateau) (Diester-Haass and Zahn, 1996; Bohaty and Zachos, 2003; Villa et al., 2008; Villa et al., 2014) has been interpreted to be a short-lived warming event in the late Eocene (~36.4 Ma).~~The generally warm conditions of the Eocene are consistent with fossil-based reconstructions of Southern Ocean circulation developed from high-latitude drill cores (Kennett, 1977; Nelson and Cooke, 2001; Kennett and Exon, 2004), in which subtropical waters are interpreted to extend close to the Antarctic margin until the late Eocene. However, both geochemical proxy data and these paleoecological reconstructions are at odds with the~~

latest generation of ocean circulation and climate modelling simulations (Hollis et al., 2012; Lunt et al., 2012). Even under hyper-greenhouse conditions, the models produce a cyclonic gyre that blocks subtropical waters from penetrating southward beyond 45°S (Huber and Sloan, 2001; Huber et al., 2004). High-latitude warmth also conflicts with evidence for the initiation of Antarctic glaciation in the latest Eocene from both fossil and geochemical proxies (Lazarus and Caulet, 1993; Scher et al., 2014; Barron et al., 2015).

Paleobiogeographic changes in marine biota may help to delineate general climate trends and events. Identifying the initial timing and development establishment of a high-latitude fauna in the Southern Ocean helps to constrain the development of the Southern Ocean frontal systems and, in turn, heat transfer between low and high latitudes. Kennett (1978) provided the first summary on the biogeographic development of planktic biota in the circum-polar Southern Ocean throughout the Cenozoic. He inferred that the development of distinct polar plankton assemblages was related to the evolution of the Antarctic Circumpolar Current (ACC) and the Antarctic Polar Front (AAPF). This change was linked by Kennett (1978) to Southern Ocean circulation changes associated with the opening of Drake Passage and Tasmanian Gateway in the late Eocene-early Oligocene and implicated as the main causal mechanisms for Antarctic glaciation. Subsequent deep-sea drilling campaigns have provided additional data on regional changes in Southern Ocean plankton, which were integrated by Lazarus and Caulet (1993) into a set of circum-polar maps across specific time intervals. Moreover, these authors also carried out the first synthesis of radiolarian biogeography for the region and found a pattern of increasing endemism in the Southern Ocean across the EOT. Nelson and Cooke (2001) undertook a comprehensive review of previous work and presented an updated synthesis on the oceanic front development in the Southwest Pacific during the Cenozoic. According to these authors, a proto-Subtropical Front was established in the late Eocene (ca. 35 Ma) and an AAPF in the early Oligocene. A more detailed study of radiolarian biogeographic patterns and trends in the Southwest Pacific was done by Lazarus et al. (2008), who found increased endemism in the radiolarian fauna in the late Eocene (ca. 35 Ma). Further radiolarian studies from the Atlantic sector of the Southern Ocean were performed by Funakawa and Nishi (2008), who recorded the first expansion of an Antarctic assemblage significantly earlier (38.5 Ma). They identified several faunal turnover events in the Antarctic assemblage from the late middle Eocene to late Oligocene and linked these events to migrations of the AAPF. Latest research suggests that the ACC was not developed

1 until ~30 Ma, together with the establishment of an AAPF (Scher et al. 2015), when the
2 Tasmanian gateway aligned with the westerly wind flow (Hill et al., 2013). From the middle
3 to late Eocene, a westward Antarctic Slope Current is inferred to have flowed across the
4 gateway, driven by the polar easterlies (Bijl et al. 2013; Scher et al. 2015).

5 ~~However, Identifying the timing of the establishment of a distinct Southern Ocean surface-~~
6 ~~water mass is inferred to have occurred within the middle to late Eocene interval, triggered~~
7 ~~by the opening of the Tasman Gateway or changes in carbon cycling (Stickley et al., 2004;~~
8 ~~Lazarus et al., 2008; Bijl et al., 2013), or abruptly at the E-O transition, associated~~
9 ~~development of a proto-Antarctic Circumpolar Current (ACC) and implicated as the main~~
10 ~~causal mechanism for Antarctic glaciation (Kennett, 1978; Nelson and Cooke, 2001; Houben~~
11 ~~et al., 2013). Improved understanding of the timing of major changes in the early Cenozoic~~
12 ~~evolution of the Southern Ocean will help to resolve the relative importance and inter-~~
13 ~~relationships between tectonism, biological evolution and long-term trends in atmospheric~~
14 ~~CO₂ concentration.~~

15 In this paper, we document variation in radiolarian assemblages and foraminiferal oxygen
16 and carbon stable isotopes from ~~the middle Eocene~~ to ~~to~~ early Oligocene ~~interval~~ (~40 to ~~33~~
17 30 Ma) at DSDP Site 277 and relate these variations to radiolarian assemblage changes at
18 DSDP ~~S~~ites 280, 281, 283 and ~~to a previously published study of Eocene radiolarian~~
19 ~~assemblages from~~ ODP Site 1172 ~~(Suzuki et al., 2009)~~. DSDP Site 277 provides a unique
20 record of pelagic sedimentation in the Southwest Pacific ~~from the~~ during late Paleocene to
21 Oligocene times and the first Eocene ~~benthic foraminiferal~~ $\delta^{18}\text{O}$ record was generated from
22 this site (Shackleton and Kennett, 1975). ~~We use these data to test if (i) a distinct Southern~~
23 ~~Ocean fauna was established prior to the major shift in oxygen isotopes in the earliest~~
24 ~~Oligocene and (ii) if tropical subtropical conditions persisted in the Southwest Pacific until at~~
25 ~~least the late Eocene. Although Lazarus et al.'s (2008) study of radiolarian assemblages~~
26 ~~included all above mentioned DSDP sites, this new work includes a more thorough~~
27 ~~taxonomic review of the radiolarian assemblages at these sites and integrates the radiolarian~~
28 ~~assemblage trends with new stable isotope data for Site 277. Our results~~ will help to identify
29 the extent to which tropical or warm-subtropical conditions prevailed during the middle and
30 late Eocene, refine the timing and nature of the development of a distinctive Southern Ocean
31 radiolarian fauna and discuss implications for the ~~oceanographic history of the~~
32 SWpaleoceanography of the Southwest Pacific from the middle Eocene to early Oligocene.

2 Study Sites

Deep Sea Drilling Project (DSDP) sites 277, 280, 281 and 283 were drilled during DSDP Leg 29 (Kennett et al., 1975) (Figure 1). The main focus of our study is Site 277, which is located on the western margin of the Campbell Plateau (52°13.43'S; 166°11.48'E) at a water depth of 1214 m. Forty-six cores were drilled with a maximum penetration of 472.5 meters below sea floor (mbsf), but with total length of 434.5 m of cored section and only 59.6% recovery. Poor recovery was due to 9.5 m coring runs being conducted every 19 m (i.e. alternate drilling and coring at 9.5 intervals) between 301.5 and 368.0 mbsf. Below 10 mbsf, a Paleogene sequence spanning from the ~~middle-late~~ Paleocene to middle Oligocene was recovered (Kennett et al., 1975). We studied Cores 277-35R (349.2 mbsf) to 277-15R (134.5 mbsf) that cover a middle Eocene-to-lower Oligocene interval. The sediment at Site 277 (paleolatitude ~~~60~~⁵⁵S) throughout the succession is highly calcareous indicating a depositional environment well above the lysocline, with a paleodepth estimated at around 1500 m (Kennett et al., 1975; Hollis et al., 1997).

~~Three-Four~~ additional sites were included in our study in order to acquire a regional picture of radiolarian assemblage change and biogeography during the middle Eocene to early Oligocene (Figure 1). DSDP Site 280 comprises two holes (48°57.44'S; 147°14.08'E) ~~and is~~ located ~100 km south of the South Tasman Rise and ~~was~~ drilled at a water depth of 4176 m. We collected radiolarian assemblage data from Hole 280A, which consists of a 201 m cored section that includes a 97.2 m middle Eocene-to-middle Oligocene interval. The studied interval spans Core ~~280A-7R~~ (123.4 mbsf) to Core ~~280A-5R~~ (92.54 mbsf). DSDP Site 281 on the South Tasman Rise (47°59.84'S; 147°45.85'E), drilled at a water depth of 1591 m, encompasses two holes (281 and 281A). We examined Hole 281 which was cored to 169 mbsf and recovered a 105.6 m (62.5% recovery) ~~late-upper~~ Eocene-to-Pleistocene section. The studied interval covers Core ~~281-16R~~ (149 mbsf) to Core ~~281-14R~~ (122.5 mbsf). DSDP Site 283 lies in the Central Tasman Sea (43°54.6'S; 154°16.96'E) ~~in-at~~ a water depth of 4729 m and also comprises two holes (283 and 283A). We examined Hole 283 which was drilled to 156 mbsf (39% recovery) and recovered a Paleocene-to-Pleistocene section that contains ~~an late-upper~~ Eocene-to-~~possible (?)~~ Miocene hiatus. Samples from Core 283-8R (192.25 mbsf) to Core 283-5R (87.75 mbsf) were studied from this site. ODP Site 1172 is situated west of the East Tasman Plateau (43°57.58'S; 149°55.69'E) in a water depth of 2622 m and was drilled during ODP Leg 189 (Exon et al., 2004). It comprises four holes (1172A, 1172B,

1172C and 1172D). The examined samples were from Section 1172A-39X-1 to Section 48X-CC (354.625–450.55 mbsf), spanning a middle Eocene-to-lower Oligocene interval, and from Section 1172D-2R-2 to Section 1172D-2R-3 (355.225–356.875), covering a lower Oligocene interval.

3 Material and methods

3.1 Sample preparation and analysis

This study is based on ~~28–33~~ sediment samples from DSDP Site 277 ~~from~~ (~350 to 135 mbsf) spanning a middle Eocene-to-lower Oligocene interval (17 reported by Hollis et al. (1997) and ~~44–16~~ new samples), 6 samples from DSDP Site 283 (new, all from the DSDP/ODP Micropaleontology Reference Centre (MRC)), 7 from DSDP Site 281 (3 from the DSDP/ODP MRC, 4 new) and 4 from DSDP Site 280 (new). Due to incomplete core recovery in all study sections, the sampling resolution of our study is variable (~0.5 to ~30 m sample spacing; ~~Supplementary Data~~). To obtain a consistent taxonomic identification across all sites, all samples previously reported from DSDP sites 277, 280, 281 and 283 were re-examined and re-counted as part of this study. The Supplementary files include taxonomic notes for all radiolarian species recorded in this study, plates of selected species, and radiolarian distribution charts and sample information for DSDP sites 277, 280, 281 and 283 (Supplementary Tables 1–5). Radiolarian census data of 41 samples from ODP Site 1172, covering a middle Eocene-to-lower Oligocene interval, are provided in the Supplementary Table 6. The radiolarian taxonomy, sample preparation and analysis methodology were published in Suzuki et al. (2009).

For strewn slide preparation, ~~1–~~10 g of sample material was broken into ~5 mm-diameter chips and ~~leached in~~acidified with 10% HCl to dissolve carbonate ~~until the reaction ceased~~. Samples were then washed through a 63- μ m sieve, and the >63- μ m residue was cleaned by gently heating in a 1:1 solution of 10% hydrogen peroxide and sodium hexametaphosphate ((NaPO₃)₆). The residue was washed though a 63- μ m sieve and dried. Dependent on the volume of the processed residue and the abundance of radiolarians, ~~1–~~5 strewn slides were prepared for each sample. If the radiolarians were sparse, specimens were individually picked from the dried residue under a stereo microscope. For strewn slides, a known portion of dried residue was evenly distributed on a pre-glued coverslip, which was inverted and placed

Formatted: Heading 2

gently on a glass slide with a thin coating of Canada Balsam. The slide was placed on a hot plate until the balsam was fixed.

Strewn slides were examined using a Zeiss transmitted light microscope fitted with a Zeiss AxioCam ERc5s digital camera. ~~The Supplementary files include taxonomic notes for all radiolarian species recorded in this study, plates of selected species, and radiolarian distribution charts and sample information for DSDP sites 277, 280, 281 and 283.~~ Radiolarian census data were derived along vertical slide traverses under transmitted light following the method of Hollis (2006). For samples with sparse radiolarians (<300 specimens per slide), all radiolarians on the prepared slide(s) were counted. For richer samples, all specimens were counted until a total number of ~~about ~~~300 specimens was achieved. The proportion of the slide examined to this point was determined and the abundance of common taxa (>15 observed specimens) estimated for the rest of the slide. The remaining portion was then examined and rare taxa (<15 specimen observed in initial count) recorded. All intact tests were assigned to a counting group that range from undifferentiated order (e.g. Nassellaria undet.) and family (e.g. Actinommidae undet.) to species and subspecies. This approach allows for an accurate estimate of the abundance of individual species, but does result in overall diversity being underestimated.

Radiolarian abundance was calculated using the following equation:

$$(X_R \times X_S \times \frac{1}{X_P}) \div A_{Sed} \quad \text{-----} \quad (1)$$

With X_R being the total number of radiolarians per slide, X_S the number of slides made of a known portion X_P of the dried material, A_{Sed} is the initial amount of dried sediment.

Additional data derived for each sample assemblages includes taxic richness, the Fisher α Diversity index and the Simpson index of Evenness. The latter two indices were calculated using the PAST software [version 3.07](#) (Hammer et al., 2001). The Fisher α index is a general guide to diversity, calculated from the number of taxa and the total number of individuals. The Simpson index of Evenness determines the degree to which assemblages are dominated by individual taxa and ranges from 0 to 1. ~~Since taxic richness is correlated to preservation and is also dependent on the sample size, we performed an individual rarefaction analysis for Site 277 samples with PAST (Supplementary Table 2). This allows the comparison of taxonomic diversity in samples of different sizes. We used 100, 200, 300 and 500 counts as sample sizes, respectively, to calculate taxic richness. Additionally, we derived a range-~~

through taxic richness after subsampling for Site 277 with R version 3.1.3 (www.r-project.org) (Supplementary Table 2). We chose sample sizes of 100 and 300, respectively, both with a subsampling of 1000. This approach shows if a diversity drop in the middle of a series is a true diversity drop or a temporary absence due to preservation. The diatom/radiolarian (D/R) ratio was calculated using the counts of diatoms and radiolarians of one examined slide. In case of very rare diatoms, all specimens were counted on a slide, otherwise several transverses were counted for diatoms and the total number estimated for the whole slide. Although this method is not an accurate measure of total diatom abundance as most pelagic diatoms are smaller than the 63- μ m screen used in this study, it serves to identify the order of magnitude in changes in diatom abundance that allows us to identify significant diatom event horizons.

3.2 Radiolarian biogeographic affinities

The assignment of biogeographic affinities ~~of the to~~ radiolarian species, subspecies and informally defined morphotypes encountered in our study is based on a comprehensive literature review. We focussed on published records of these taxa or their close relatives from the Southwest Pacific and Southern Ocean (e.g. Petrushevskaya, 1975; Takemura and Ling, 1997; Sanfilippo and Caulet, 1998; Hollis, 2002; Funakawa and Nishi, 2005; Hollis et al., 2005; Hollis, 2006; Funakawa et al., 2006; Funakawa and Nishi, 2008; Kamikuri et al., 2012). This literature review was complemented with radiolarian occurrence data from the NSB (Neptune Sandbox Berlin) Database (Lazarus, 1994; Spencer-Cervato, 1999). Unfortunately, this database lacks many Paleogene radiolarians, and, for those that are present, occurrences need to be cross-checked with the DSDP/ODP reports. The first step was to assess the paleolatitude of each site for the interval of radiolarian ranges. We used www.paleolatitude.org (van Hindsbergen et al., 2015) to extract paleolatitude information in intervals of 10 Ma for the past 60 Ma and created the mean value for each site for an age range (Supplementary Table 11). We listed radiolarian taxa and their range and abundance at high-latitude (>45°N/S), mid-latitude (25–45°N/S) and low-latitude sites (0–25°N/S) and observed that presence/absence data are not always a reliable guide to biogeographic affinity (Supplementary Table 12). For instance, *Lithomelissa ehrenbergi* (Buetschli 1882) was described from Barbados, which may indicate that this species has a tropical or cosmopolitan ecology. However, the species is far more abundant at high-latitude sites, and only rarely recorded at low-latitude sites. Moreover, Haeckel (1887) found recent *L. ehrenbergi* from

Formatted: Heading 2

1 deep-water samples at low latitudes. Therefore, we interpret this species as a cold-water
2 indicator, commonly found in high-latitude samples and sometimes found in deep-water
3 samples in low latitudes. The biogeographic affinities of *Amphicraspedum murrayanum* and
4 *A. prolixum* group also warrant some discussion. These taxa are widely reported in early and
5 middle Eocene sediments but occur in greater abundance in the Southwest Pacific at times of
6 global warmth (Hollis, 2006). Liu et al. (2011) suggested that these taxa were not valid
7 indicators of high-latitude warming because they are found in the Paleocene in the North
8 Atlantic. However, their assumption that Southwest Pacific and North Atlantic Ocean
9 conditions would have been similar in the Paleogene is not supported by ocean circulation
10 models (Huber et al., 2003, 2004). These models indicate that oceanic conditions for the
11 North Atlantic and the Southwest Pacific were substantially different in the early Paleogene:
12 the North Atlantic was bathed in warm currents of ~25°C moving northwards (Huber et al.,
13 2003), while the Southwest Pacific was influenced by a strong cyclonic gyre preventing
14 warm waters from penetrating southwards, except during times of extreme global warmth
15 (Huber et al., 2004; Hollis et al. 2012). Thus, the occurrence of warm-water indicators
16 throughout the Paleocene-Eocene interval in the mid-latitude North Atlantic is consistent
17 with both the global circulation model results and our interpretation of influxes of
18 *Amphicraspedum* as being indicative of warming. ~~were assigned using information from~~
19 ~~previous paleobiogeographic studies (Lazarus and Caulet, 1993), distributions reported in~~
20 ~~taxonomic studies (Petrushevskaya, 1975; Sanfilippo and Caulet, 1998) and our own~~
21 ~~assessment based on published records of the recorded taxa or closely related taxa (e.g.~~
22 ~~Takemura and Ling, 1997; Hollis, 2002; Funakawa and Nishi, 2005; Funakawa et al., 2006;~~
23 ~~Funakawa and Nishi, 2008; Kamikuri et al., 2012) (Table 1). We quantified trends in~~
24 ~~biogeographic affinity to determine how the relative influences of high and low latitude~~
25 ~~water masses varied through the middle Eocene to early Oligocene.~~

26 Tectonic reconstructions of the Australia-Antarctica-Pacific plate circuit were undertaken in
27 GPlates version 1.5 (Boyden et al. 2011) using finite poles of rotation for the relative motions
28 between: Australia-East Antarctica from Cande and Stock (2004) (0–38.13 Ma); East
29 Antarctica-West Antarctica from Granot et al. (2013) (30.94–40.13 Ma); and West
30 Antarctica-Pacific from Croon et al. (2008) (0–47.54 Ma). Relative motions of the Australia-
31 Antarctica-Pacific plate circuit were tied to the Australian paleomagnetic apparent polar
32 wander path of Torsvik et al. (2012) to provide an estimate of paleolatitude appropriate for

paleoclimate studies (van Hinsbergen et al., 2015). The 2000 m isobath from the GEBCO bathymetric grid (www.gebco.net) was used to approximate continental boundaries. The continental/oceanic boundaries of Bird (2003) are also shown (dashed lines in Figure 1 and 8) for regions where extension has significantly thinned continental crust. Each DSDP and ODP study site was assigned to the appropriate plate for reconstruction.

The overlap of the North and South Islands of New Zealand in these reconstructions is a consequence of the finite poles of rotation determined from the Adare Trough by Granot et al. (2013), which constrain the motion of East and West Antarctica between 40 and 30 Ma. These new poles result in a poor fit (significant overlap) of continental crust between the two islands that is not supported by geological data. The discrepancy between geological and paleomagnetic data could be reconciled with the use of seafloor spreading data from the Emerald basin (e.g. Keller, 2003), which describes Australia-Pacific relative motions (Sutherland, 1995) between 40 to 30 Ma, and the Adare Trough. However, our sites lie south of New Zealand and so we make no attempt to resolve this issue here.

3.3 Stable isotope analysis

At the University of California Santa Cruz (UCSC) and the University of Southampton (UoS), stable oxygen ($\delta^{18}\text{O}$) and carbon ($\delta^{13}\text{C}$) isotope ratios measurements of foraminiferal samples from Site 277 were determined-conducted in the stable isotope laboratories at the University of Southampton (UoS) and University of California Santa Cruz (UCSC). Sample analyses included for bulk carbonate, benthic foraminifera (*Cibicidoides* spp.), and the planktic foraminifera *Subbotina* spp. (thermocline) (Core 277-34R (from 332.62–159.88 mbsf) to 18R (159.88 mbsf) and *Globigerinatheka* index (mixed layer) (Core 277-34R (from 332.62–188.58 mbsf) up to (its last occurrence) in Core 277-21R (188.58 mbsf)). In total, set of 157–169 samples spanning the middle Eocene-to-lower Oligocene interval of DSDP Hole 277 was-were measured (Supplementary Tables 7–10). ~~Stable isotope analyses at UCSC were performed on a VG Prism dual-inlet mass spectrometer coupled to carousel preparation device with common acid bath maintained at 90°C. Analyses-~~ Stable isotope analyses at the UoS were performed on a Europa GEO 20-20 dual-inlet mass spectrometer with CAPS preparation oven maintained at 70°C. ~~and Stable isotope analyses at UCSC were performed on a VG Prism dual-inlet mass spectrometer coupled to carousel preparation device with common acid bath maintained at 90°C.~~ All values are reported relative to the Vienna Pee Dee

Formatted: Heading 2

Belemnite (VPDB) standard. In both labs, analytical precision, based on replicate analyses of in-house marble standards and NBS-19 averaged $\sim 0.0507\%$ (1σ) for $\delta^{13}\text{C}$ and $\sim 0.08\%$ (1σ) for $\delta^{18}\text{O}$. ~~All planktic foraminifera in this record appeared to have a 'frosty' preservation.~~

4 Results

4.1 Site 277 biostratigraphy and stable isotope stratigraphy

Broad age control for DSDP Site 277 is based on the biostratigraphic ~~review-synthesis~~ of Hollis et al. (1997) who correlated the succession to Southern Hemisphere (SH) radiolarian Zones RP6 to RP15. In this study we confirm the location of the base of ~~Zone RP12(SH)~~ (Lowest Occurrence [LO] of *Lophocyrtis longiventer*) at 371.2–349.2 mbsf, the base of RP14(SH) (Lowest Occurrence [LO] of *Eucyrtidium spinosum*, 38 Ma) at 264.5–254.5 mbsf, the base of RP15(SH) (LO of *Eucyrtidium antiquum*) at 197.8–186.5 mbsf, and the base of upper Zone RP15(SH) at 143.9–134.5 mbsf (lowest-Lowest common-Common occurrence Occurrence [LCO] of *Axoprunum? irregularis*) (Figure 2). We revise the base of Zone ~~RP12~~ to 371.2–349.2 mbsf (LO of *Lophocyrtis longiventer*) and the base of RP13(SH) to 313.5–312.7 mbsf (LOs of *Eusyringium fistuligerum* and of *Zealithapium mitra*) (Figure 2). The Eocene-Oligocene boundary is poorly defined by biostratigraphy at DSDP Site 277. Further refinement of the age control for Site 277 is possible through application of several additional bioevents, which help to correlate the discontinuous stable isotope record of this site to those from other Southern Ocean sites (Figure 2). The base of the local New Zealand stage Kaiatan is defined by the Highest Occurrence [HO] of *Acarinina primitiva* (Morgans 2009) occurring at 280–273 mbsf based on Jenkins (1975) (39.1 Ma; Raine et al., 2015). We set the base of the Kaiatan at 276.5 mbsf to allow for the correlation between isotope records (Figure 2). The base of the local Whaingaroan Stage (latest Eocene, 34.6 Ma; (Raine et al., 2015)) is identified by the ~~Highest Occurrence [HO]~~ of *Globigerinatheka index*; ~~This-this~~ event was identified at 189.6 mbsf by Jenkins (1975) but in the course of preparing foraminifera for stable isotope analysis we have determined that the event occurs slightly higher at 188.58–187.5 mbsf. The base of nannofossil zone NP17 (LO of *Chiasmolithus solitus*, 40.4 Ma; Gradstein et al., 2012) is placed at 312.5–301.5 mbsf (Edwards and Perch-Nielsen, 1975). The LCO of *Chiasmolithus oamaruensis*, 37.32 Ma (Gradstein et al., 2012), defines the base of NP18 at 244.5–240.6 mbsf (Edwards and Perch-Nielsen, 1975). The base of NP19–20 is

Formatted: Font: Italic

defined by the LO of *Isthmolithus recurvus*, 36.97 Ma (Gradstein et al., 2012) at 226.58–225.5 mbsf (Edwards and Perch-Nielsen, 1975). Within NP19-20, the HO of *Criboecentrum reticulatum* is found at 206.5–201.1 mbsf (Edwards and Perch-Nielsen, 1975), estimated at 36.44 Ma (Raine et al., 2015). The base of NP21-22 (HO of *Discoaster saipanensis*) is placed at 191.6–190.1 mbsf (Edwards and Perch-Nielsen, 1975) and is dated at 34.44 Ma (Gradstein et al., 2012). As *D. saipanensis* is a warm-water taxon, its disappearance is likely to have occurred earlier at high latitudes. The Eocene-Oligocene boundary is approximated by the HO of *G. index* at DSDP Site 277. More precise location is complicated by incomplete recovery and the highly disturbed nature of Cores 277-19R, 20R, and 21R.

Further refinement of the age control for Site 277 is possible through correlation of the stable isotope records to those from other Southern Ocean sites (Figure 2). Although the recovery gaps in the Site 277 stable isotope record preclude detailed correlation, the broad trends and major events such as the MECO (~40 Ma) and PrOM event (~37.3 Ma) can be identified in the benthic $\delta^{18}\text{O}$ and $\delta^{13}\text{C}$ isotope profiles and compared to the middle Eocene-to-early Oligocene benthic isotope stratigraphy from ODP Site 689 (Maud Rise; Diester-Haass and Zahn, 1996) (Figure 2). The EOT interval is expressed as characterized by a large (~1‰) positive shift in benthic oxygen and carbon isotopes between Cores 277-20R and -19R (183.64–171.28 mbsf) (Shackleton and Kennett, 1975; Keigwin, 1980), which is slightly lower than the full magnitude of the benthic $\delta^{18}\text{O}$ shift seen at other Southern Ocean sites on the Kerguelen Plateau and Maud Rise (Diester-Haass and Zahn, 1996; Zachos et al., 1996; Bohaty et al., 2012).

4.2 Site 277 oxygen and carbon isotopes

Site 277 Foraminiferal $\delta^{18}\text{O}$ values results show a normal typical planktic-benthic surface-to-deep gradient with more positive-negative values in bulk and planktic foraminifers compared to the benthic foraminifers compared to bulk and planktic foraminifera with some crossover in the latter two (Figure 3, Supplementary Tables 7–10). Foraminiferal $\delta^{13}\text{C}$ values also show a typical positive benthic-planktic display typical gradients, with more positive values in bulk and planktic foraminifers compared to benthic foraminifers (Figure 3). Therefore, we interpret relatively robust stable isotope signals representative of deep (intermediate), upper (thermocline) and uppermost (mixed/surface) waters. However, all planktic foraminifera analysed from Site 277 are characterized by a ‘frosty’ preservation state, indicating some

Formatted: Heading 2

~~diagenetic alteration although it is likely that the $\delta^{18}\text{O}$ gradients are attenuated by diagenetic effects on planktic foraminifera (Sexton et al., 2006). We have therefore focused our interpretation on benthic foraminifera because their isotopic signatures are likely less affected by diagenesis, as they show a ‘frosty’ preservation.~~

Several short-lived climatic events are identified in the benthic stable isotope records at Site 277 (Figures 2 and 3, Supplementary Table 7). The body of the MECO was not recovered (due to a 16-m sampling gap between the top of Core 277-33R and the base of Core 277-32R), but MECO's onset and recovery is well constrained by a 0.5‰ negative excursion shift in benthic $\delta^{18}\text{O}$ values at ~313 mbsf (between Samples 277-33R-2, 106–108 cm and -33R-1, 129–130.5 cm) and a ~0.4‰ positive excursion shift in $\delta^{18}\text{O}$ values at ~296 mbsf (between samples 32R-3, 107–109 cm and 32R-3, 77–79 cm), indicating that the MECO spans ~17 m (Figure 2). The MECO is more strongly expressed in the benthic $\delta^{18}\text{O}$ than in the planktic record but this may relate to the poor recovery of the body of the event at this site or diagenetic impacts on planktic $\delta^{18}\text{O}$ values (Pearson et al., 2000, 2001; Sexton et al., 2006). In agreement with other records (Bohaty and Zachos, 2003; Bohaty et al., 2009), a positive $\delta^{13}\text{C}$ excursion shift is observed in conjunction with the onset of the MECO in the benthic and bulk carbonate records (Figure 2), although the $\delta^{13}\text{C}$ record is also compromised by the missing core of the event.

The PrOM event (Scher et al., 2014) is well-defined in the $\delta^{18}\text{O}$ record from DSDP Site 277 but also spans two three significant recovery gaps between at the base of Cores 277-26R, 25R and 24R (~244.5 to 225.5 mbsf) (Figure 3). The ~0.4‰ positive shift in $\delta^{18}\text{O}$ that marks the onset of the PrOM, spans upper Core 277-26R and lower Core 277-25R (~240–230 mbsf), and is followed by an interval of relatively low $\delta^{18}\text{O}$ values in upper Core 277-25R, prior to reaching maximum values in uppermost Core 277-25R (~226 mbsf) (Figure 2). A gradual decrease in $\delta^{18}\text{O}$ occurs through Core 277-24R. We define the PrOM at DSDP Site 277 as the interval within these three cores in which benthic $\delta^{18}\text{O}$ exceeds 4.25–0.6‰, with the exception of the interval noted above a narrow interval in upper Core 277-25R. These benthic $\delta^{18}\text{O}$ values are lower than those reported by Scher et al. (2014), but it is likely that peak $\delta^{18}\text{O}$ values are not captured at Site 277. Consequently the PrOM is placed between 240.62 and 219.57 mbsf (spanning a ~21-m section). The planktic $\delta^{18}\text{O}$ records show is similar trends to the benthic record in the PrOM interval, but lacks the maximum excursion in uppermost Core 277-25R. At the onset of the PrOM event, short-lived negative $\delta^{13}\text{C}$ excursions are evident in

the benthic, bulk and planktic records. However, a longer-term positive trend for planktic and benthic $\delta^{13}\text{C}$ values ~~becomes apparent simultaneously to~~ is associated with the benthic $\delta^{18}\text{O}$ maximum.

Directly above the PrOM event, there is a short-lived ~0.4‰ decrease in $\delta^{18}\text{O}$ values decrease by -0.5‰ in upper Core 277-24R and -23R (217.37-210.74 to 207.41 mbsf), evident in benthic and planktic foraminifera as well as bulk carbonate, prior to the increase in $\delta^{18}\text{O}$ that spans the EOT (Figure 3). Benthic and planktic $\delta^{13}\text{C}$ also exhibit a small negative excursion at this level. This interval ~~can~~ may be correlated to the late Eocene warming interval ~~interpreted-reported from~~ ODP ~~S~~ sites 689 (Maud Rise), 738, 744, and 748 (Kerguelen Plateau) (Diester-Haass and Zahn, 1996; Bohaty and Zachos, 2003; Villa et al., 2008; Villa et al., 2014).

~~The~~ A large positive shift in $\delta^{18}\text{O}$ ~~defines the E-O transition~~ occurs at Site 277 between the base of Core 277-20R and Core 277-19R, with ~~the most positive~~ maximum values in benthic and planktic $\delta^{18}\text{O}$ and $\delta^{13}\text{C}$ occurring in Core 277-19R (171.28 to 169.65 mbsf), ~~within the earliest Oligocene.~~ This can be correlated to the large $\delta^{18}\text{O}$ shift across the EOT documented at many deep-sea sites, which is characterised by two distinct steps (EOT-1 and Oi-1) in more complete sections (e.g., Coxall et al., 2005; Katz et al., 2008).

We note that the stable isotope record at Site 277 exhibits high amplitude cyclical variation in the range of 0.5‰ for benthic $\delta^{18}\text{O}$ and slightly more for $\delta^{13}\text{C}$ (Figure 3). The presence of at least 10 cycles within the 6 million years between the MECO and the EOT is consistent with orbital-scale forcing. Although the record is too incomplete to establish the frequency of these cycles, their presence in this expanded Paleogene section bodes well for future drilling at this location.

4.3 Radiolarian assemblages at DSDP Site 277

In total, 16 families, 56 genera and 98 radiolarian species were identified at DSDP Site 277 (Supplementary Table 1). Radiolarian abundance is generally low (10–100 specimens/g) and preservation is moderate throughout the middle Eocene-to-~~early-late~~ lower upper Eocene interval (349.2 to 227.2 mbsf) (Figure 4). In the ~~latest-uppermost~~ Eocene and ~~lower~~ early Oligocene (206.83–143.9 mbsf) radiolarians are abundant to very abundant (>1500 specimens/g) and well preserved. Diversity increases during the MECO (313.5–296 mbsf) and in the upper Eocene (226.10–186.5 mbsf) and drops in the lower Oligocene (162.2–134.5

Formatted: Font: Not Bold

mbsf) (Figure 4). A short-lived drop in radiolarian abundance (<500 specimens/g) and diversity is observed at 210.5–207.5 mbsf during the late Eocene warming event. Diversity is strongly correlated to closely parallels trends in abundance and preservation, which is lower in the middle and early late Eocene and high thereafter (Figure 4). Simpson Evenness is strongly correlated to with diversity but exhibits greater troughs where samples are sparse (Figure 4). Spumellarians are dominant in most samples ranging between ~45–44 and 96% (~70–71% average). The main families are the Actinommidae, Litheliidae, Spongodiscidae, Artostrobiidae, Spongodiscidae, Lychnocaniidae and Lophocyrtidae and Lychnocaniidae (Supplementary data table Site 277 Table 1).

Three samples from the middle Eocene section of Site 277 (313.5 mbsf, 312.7 mbsf, 296 mbsf; Cores 277-32R and -33R) that lie within the onset and recovery of the MECO at Site 277, show improved preservation, a peak in diversity, and mark the first significant occurrence of diatoms (Figure 4). The low-latitude species *Amphymenium* *Amphicraspedum murrayanum* and *Amphycraspedum* *A. prolixum* gr. have short lived isolated occurrences in this interval, with while only *A. prolixum* gr. also has trace occurrences in five samples very rare in the latest uppermost Eocene to lowermost Oligocene (Cores 277-24R to -20R at 217.70 mbsf, 209 mbsf, 207.5 mbsf, 197.82 mbsf and 186.50 mbsf). Several species are restricted to the MECO, including: *Artobotrys titanothericeraos*, *Sethocyrtis chrysallis*, *Eusyringium fistuligerum* and *Stichopilium* cf. *bicorne*. *Lophocyrtis jacchia hapsis*, which is a high-latitude variant of *L. jacchia jacchia* (Sanfilippo and Caulet, 1998) and endemic to the Southern Ocean, is also common during the MECO and uppermost Eocene (217.7–206.83 mbsf), but is absent from the remaining middle and lower upper Eocene and very rare in the late Eocene. Furthermore, the LOs of several (albeit rare) species are recorded (albeit very rare) at this site during the MECO interval (*Axoprunum pierinae*, *Zealithapium mitra*, *Periphaena* spp., *Larcopyle hayesi*, *L. polyacantha*, *Zygocircus buetschli*, *Siphocampe?* *amygdala*, *Eucyrtidium ventriosum* *montiparum*, *Lychnocanium amphitrite*, *Clinorhabdus anantomus*, *Lophocyrtis keraspera*, *Lophocyrtis dimitricai*, *Cryptocarpium ornatum* and *Lamprocyclas particollis*) (Figure 2 and Supplementary data table Site 277 Table 1).

A major change in siliceous assemblages occurs within the PrOM interval (~226 mbsf; Core 277–25R), coincident with maximum values in benthic $\delta^{18}\text{O}$ (Figure 4). A pronounced increase in radiolarian abundance (from <50 to ~4000 radiolarians/gram), preservation and diversity occurs at 226.10 mbsf (Sample 277-25R-1, 60 cm). Diatoms also become abundant

Formatted: Font: Not Italic

at the same level as the increase in radiolarian abundance. The most abundant nassellarian families are the Artostrobiidae (~22%), Lophocyrtiidae (~6%) and Lychnocaniidae (~2.5%). Plagiacanthidae account for ~2%. The following taxa have their LO within the PrOM at Site 277: *Lithelius* (?) *foremanae*, *Ceratocyrtis* spp., *Lithomelissa ehrenbergi*, *L. gelasinus*, *L. sphaerocephalis*, *Siphocampe nodosaria*, *Artostrobos annulatus*, *Artostrobos* cf. *pretabulatus*, *Clathrocyclas universa*, *Dictyophimus*? aff. *archipilum*, *Lychnocanium waiareka*, *Aphetocyrtis rossi* and *Theocyrtis tuberosa* (Figure 2 and Supplementary data table Site 277 Table 1). ~~Diatoms become abundant at the same level as the increase in radiolarian abundance and remain abundant through the latest Eocene, decreasing in the Oligocene.~~

~~Five samples were investigated at Site 277 that lie within the late Eocene warming event (210.5–207.5 mbsf). During this event, radiolarian abundance and diversity decrease significantly, as well as diatom abundance (Figure 4). The radiolarian assemblages of these five samples differ from the other uppermost Eocene samples. Lychnocaniidae are more abundant (~12%), whereas Artostrobiidae are absent. Furthermore, Lophocyrtiidae decrease (~4%) and Plagiacanthidae and *Larcopyle* spp. are very rare (0.5% and 0.9%, respectively; Supplementary Table 1).~~

~~Immediately after the warming event, a second pronounced increase in radiolarian abundance (from <200 to 9600 specimens/gram) and diversity is observed at 206.83 mbsf, together with an increase in diatom abundance (Figure 4). In the uppermost Eocene-to-lowermost Oligocene interval (206.83–186.5 mbsf), Plagiacanthidae (~5%), Artostrobiidae (~7%) and Lophocyrtiidae (~10%) increase again, whereas Lychnocaniidae decrease (~2%; Supplementary Table 1).~~

~~The most abundant radiolarian families in the PrOM and latest Eocene are the Actinomiidae (~11–36%), Litheliidae (~16–28%), Spongodiscidae (~5–13%), Lophocyrtiidae (~3–15%), Lychnocaniidae (1–11%) and Plagiacanthidae (1–6%). *Theocyrtis tuberosa* has a very rare occurrence from the late-upper Eocene to early-lower Oligocene (~226–143.9 mbsf; Core 277-25R to 16R). This species is also known to have had isolated occurrences in the southern Atlantic and southern Indian oceans in the late Eocene (Takemura, 1992; Takemura and Ling, 1997) and is common in latest Eocene to early late Oligocene assemblages from low to middle latitudes of all ocean basins (Sanfilippo et al., 1985). As none of our samples lie within the late Eocene warming interval (Figure 3), we cannot assess how radiolarian assemblages responded to this warming. However, closer to New Zealand, the latest Eocene~~

~~Runangan stage is associated with incursions of warm water taxa, including larger benthic foraminifera and the short-lived occurrence of the low-latitude genus *Hantkenina* (Hornibrook et al., 1989).~~

A significant decline in radiolarian abundance and diversity is observed through the ~~early~~ lower Oligocene (186.5 to 134.5 mbsf; Cores 277-20R to -15R) (Figure 4). Radiolarian abundance declines from 6400 to 750 radiolarians/gram. Many nassellarian taxa decline or disappear, especially within the Lophocyrtidae and Plagiacanthidae. The fauna is dominated by spumellarians thatSpumellarians increase from ~73% to ~97% of the total fauna, with Litheliidae and Actinommidae being the most abundant families (Supplementary ~~data table~~ Site 277Table 1).

Rarefaction analysis of Site 277 radiolarian data (Figure 4) indicate that counts of at least 300 specimens are required to achieve a reliable measure of diversity and taxic richness. However, poor preservation in the middle Eocene and lower upper Eocene intervals (~350 to ~227 mbsf) has resulted in poor recovery of radiolarians with 9 samples containing <300 specimens and 9 samples of <100 specimens. Because these samples span an interval in which significant changes in diversity and assemblage composition occur, we include metrics for all samples in Figure 4 (samples of <100 specimens, <300 specimens and >300 specimens are highlighted) and metrics for samples with >100 specimens in Figures 6 and 7. To investigate whether the diversity drop between ~292 to ~227 mbsf is a preservational artefact or a real feature of the assemblage, we also determined range-through taxic richness (Figure 4). We have chosen sample sizes of 100 and 300 (both with a subsampling of 1000), respectively, which show a similar pattern to the original observation. The decrease in range-through taxic richness at the top and bottom of the record is due to edge effects. According to this analysis, range-through taxic richness is higher than observed in Core 277-32 to -26 (292.2–235.5 mbsf). Chert nodules are present down-core from ~246 mbsf, so the scarcity of taxa in the interval between ~350 and 246 mbsf is likely to be an artefact of diagenesis. However, the increase in taxic richness in the MECO appears to be supported by this analysis, at least for the uppermost sample. The analysis also indicates that there is a distinct increase in diversity related to the PrOM event around ~226 mbsf, although it is more muted than the raw data suggest. It is notable that the decrease in diversity evident in the raw data during the late Eocene warming event is not shown in the range-through data. In fact, there may be a further increase in taxic richness within this interval. We conclude that range-

through taxic richness is a helpful tool for determining if diversity changes are due to diagenesis or environmental variation, especially when coupled with consideration of the lithologic changes (e.g. chertification).

4.4 Radiolarian assemblages at other ~~SW~~Southwest Pacific sites

To establish the significance and nature of radiolarian faunal turnover associated with the PrOM event regionally, we investigated the ~~late-upper Eocene-Eocene-to-to-early-lower~~ Oligocene intervals of DSDP ~~S~~sites 280, 281 and 283 and ODP Site 1172.

4.4.1 DSDP Site 280

Four samples were investigated at DSDP Site 280 from Cores ~~280-~~7R, 6R and 5R (123.4 to 92.54 mbsf). In previous work, the E-O boundary in Hole 280 was placed at the base of Core 280-6R (110.5 mbsf) (Crouch and Hollis, 1996). However, due to the presence of *Eucyrtidium antiquum* (Caulet, 1991) and *Larcopyle frakesi* (Chen, 1975), both of which have LOs in the ~~early-lower~~ Oligocene, we place the studied interval (123.4–92.54 mbsf) in ~~early-lower~~ Oligocene Zone RP15(SH) (Figure 5, ~~and Supplementary data-table Site 280Table 3~~). This is in agreement ~~with~~ O'Connor (2000), who found ~~late-upper~~ Eocene assemblages were restricted to Cores 280-10R to ~~-~~8R (205.5 to 139 mbsf). The absence of the zonal marker *Axoprunum? irregularis* indicates correlation with lower RP15(SH). *Eucyrtidium spinosum*, which according to Funakawa and Nishi (2005) has its HO in the ~~early-lower~~ Oligocene, is absent in the Site 280 study interval. However, the HO of this species is recorded within the ~~late-upper~~ Eocene interval at Site 277, suggesting a diachronous HO between the Southwest Pacific and the South Atlantic (~~Supplementary data table Site 277~~).

In total, 15 families, 35 genera and 50 radiolarian species were identified at Site 280. Radiolarians are abundant (1000–2500 specimens/g) and well preserved in all samples. Diatoms are also very abundant (D/R ratio ~10) (Figure 5). Diversity and Evenness is stable and high in all samples. Spumellarians are slightly more abundant than nassellarians (52–66% of the assemblage). The most abundant families are Litheliidae (20–37%), Plagiacanthidae (14–22 %), Actinommidae (4–12%), Spongodiscidae (5–9%), Eucyrtidae (4–8%) and Lophocyrtidae (3–8%) (~~Supplementary data-table Site 280Table 3~~). Compared to DSDP Site 277, this site has ~~a~~ higher diatom abundance and better overall preservation,

which ~~might~~ may explain the higher diversity. More species of the genera *Lithomelissa* (7) and *Larcopyle* (5) are present, as well as a higher abundance of Lophocyrtiidae. Lychnocaniids are very rare at this site (<1%) and the genus *Lychnocanium* is absent (Supplementary ~~data table Site 280~~ Table 3).

4.4.2 DSDP Site 281

Seven samples were investigated from DSDP Site 281 in the interval between 149 and 122.5 mbsf (Cores 281-16R to 14R) (Figure 5). Results from three of these samples were previously reported in Crouch and Hollis (1996) but have been re-examined for this study. Due to the presence of *Eucyrtidium spinosum* and *Eucyrtidium nishimurae*, the latter with a HO in the late Eocene at ~36.9–36.7 Ma (Funakawa and Nishi, 2005), we correlate the Site 281 study interval with lower Zone RP14(SH) (~Kaiatan local stage). A hiatus spanning the ~~latest-uppermost~~ Eocene and Oligocene is inferred from the presence of abundant glauconite in the upper part of Core 281-14R as well as from common *Cyrtocapsella tetrapera* in Core 281-13R, which indicates a Miocene age (Crouch and Hollis, 1996).

In total, 14 families, 34 genera and 46 species were identified at Site 281. Radiolarians are abundant (2000–4000 specimens/g) and well preserved. Diversity is lower than at Site 280A, but Evenness is still ~~very~~ high and similar to the other sites (Figure 5). The D/R ratio is also ~~very~~ high and comparable to Site 280, except in the upper two samples in Core 281-14R (125.5–122.5 mbsf). The radiolarian assemblages are dominated by spumellarians (55–93%), with Litheliidae (17–42%), Spongodiscidae (12–30%) and Actinommidae (10–20%) the most abundant families. The most common nassellarians belong to the Plagiacanthidae (1–15%), Lophocyrtiidae (3–7%) and Eucyrtiidae (1–7%) (Supplementary ~~data table Site 281~~ Table 4). Although ~~S~~ sites 280 and 281 were relatively close to each other (Figure 1), the radiolarian assemblages are distinctly different, indicating different oceanographic conditions. Crouch and Hollis (1996) concluded that Site 281 was shallower and closer to terrigenous influx than Site 280. The depositional environment of Site 280 is interpreted as more oceanic. The greater abundance of Spongodiscidae at Site 281 supports a shallower oceanic setting for this locality (Casey, 1993). Compared to the ~~early-late~~ early upper Eocene assemblage of Site 277, where radiolarian abundance and diversity is very low, with several samples containing less than ~100 specimens, Site 281 contains more Spongidiscidae (~20%), Plagiacanthiidae (~7%) and Litheliidae (~20%), whereas the genus *Lychnocanium* is absent at Site 281.

4.4.3 DSDP Site 283

Six samples were examined from Site 283 between 192.25 and 87.75 mbsf (Cores ~~283~~-8R to ~~5~~-5R) (Figure 5). The lowermost sample at 192.25 mbsf is correlated to RP13(SH) due to the absence of *Eucyrtidium spinosum*. The uppermost five samples are of early late Eocene age based on the presence of *E. spinosum* and nannofossil age control (Edwards and Perch-Nielsen, 1975). The age of the Site 281 and 283 successions are poorly defined and the PrOM event cannot be located at these sites. Both sites contain *Eucyrtidium nishimurae*: at Site 283 in all samples, at Site 281 its HO is in 125.5–122.5 mbsf. According to Funakawa and Nishi (2005) its HO is in C17n1n (~36.7 Ma; ~~(Gradstein et al., 2012)~~). *E. nishimurae* is absent at Site 277. The deposition of siliceous ooze in the ~~late-upper~~ middle to ~~late-upper~~ Eocene and the absence (or very rare) occurrence of foraminifera suggests a deep oceanic setting close or below the Calcite Compensation Depth (CCD) for Site 283.

A total of 16 families, 50 genera and 81 radiolarian species were recorded at Site 283. Radiolarians are ~~very~~ abundant (4700–21150 radiolarians/gram), with the highest abundance in Cores 283-6R and 5R, well preserved, and diverse (59–77 taxa per sample, Fisher α Index of 10–13, Evenness of 0.75–0.89). Diatoms are present in low abundance with D/R ratios <1 (Figure 5). Spumellarians account for 59–87 % of the assemblage, with the Litheliidae (23–38%), Actinommidae (5–19%) and the Spongodiscidae (2–8%) the most abundant families. The Trissocyclidae (2–11%), Eucyrtidae (2–11%), Lophocyrtidae (3–8%) and Plagiacanthidae (2–8%) are the most common nassellarian families (Supplementary ~~data~~ ~~table Site 283~~Table 5). *Theocyrtis tuberosa* is very abundant in the uppermost sample. The acme of this taxon might be correlated to its rare occurrence at Site 277 in the ~~late-upper~~ Eocene. Several taxa appear earlier at Site 283 than at Site 277. These include the following taxa that occur in the ~~late-upper~~ middle Eocene (e.g. *Axoprunum bispiculum*, *Amphicentria* sp. 1 sensu Suzuki, *Ceratocyrtis* spp., *Lithomelissa ehrenbergi*, *L. cf. haeckeli*, *L. sphaerocephalis*, *L. tricornis*, *Pseudodictyophimus gracilipes* gr., *Tripodiscinus clavipes*, *Siphocampe nodosaria*, *Spirocyrtis joides*, *Aspis* sp. A sensu Hollis, *Clathrocyclas universa*, *Eurystomoskevos petrushevskae*, *Lychnocanium waiareka*, *Aphetocyrtis gnomabax*) or ~~early~~ ~~late~~lower upper Eocene (*Spirocyrtis greeni*, *Eurystomoskevos cauleti*, *Lophocyrtis jacchia hapsis*, *Lamprocyclas particollis*) at Site 283.

4.4.4 ODP Site 1172

Forty ~~four-one~~ samples were ~~considered analysed~~ from ODP Site 1172 spanning ~~a-the~~ middle Eocene-to-lower Oligocene interval ~~-, including F~~four samples from ~~Hole D~~, Core 1172D-2R (356.875–355.675 mbsf) and thirty ~~six-seven~~ from ~~Hole A~~, Cores 1172A-48X to 39X (445.01–354.625 mbsf). The faunal assemblages of ODP Site 1172 were described by Suzuki et al. (2009), who did not correlate them to RP Zones. ~~We identified key radiolarian index species and correlated the interval to RP Zones 10–15. The absolute age of the succession is based on the age depth plot of Site 1172 by Stickley et al. (2004).~~ Many taxa used to define Southern Hemisphere RP zones at Site 277 are absent at Site 1172 or have diachronous ranges. ~~We place the base of Zone RP10–12 (LO of *Theocampe mongolfieri*) at 450.55–445.01 mbsf (43.14–42.79 Ma). The base of Zone RP13 (LO of *Eusyringium fistuligerum*) can be located at 419.21–417.71 mbsf (40.48–40.35 Ma), however *Zealithapium mitra* is absent. *Eucyrtidium spinosum*, the marker for Zone RP14(SH), has its LO at 373.75–371.21 mbsf (38.05–37.2 Ma) and, but *Lithomelissa tricornis* and *Pseudodictyophimus gracilipes* are absent. *Eucyrtidium antiquum* has a single LO at 365.21 mbsf (35.15 Ma), but is absent in the early Oligocene. *E. nishimurae* is present within the middle and ~~late-upper~~ Eocene. *Axoprunum irregularis* is very abundant in the lower Oligocene interval at this site (356.875–354.625 mbsf), which we correlate to the upper RP15(SH) zone.~~

Formatted: Font: Italic

Spumellarians dominate the Site 1172 assemblages throughout the middle Eocene to ~~early~~ lower Oligocene (~~~80~~82%). The Litheliidae are the most abundant family comprising about 20% on average in the middle Eocene, 35% in the ~~late-upper~~ Eocene, and 25% in the ~~early~~ lower Oligocene. Plagiacanthidae (0.5–2.5%), Eucyrtidiidae (0.5–3%), Lophocyrtiidae (1.5–8%) and Lychnocaniidae (0.5–2.7%) account for most of the nassellarians. Fisher α Diversity and Simpson Evenness are very high throughout the succession, ranging between ~10–20 and 0.82–0.96, respectively. Similar to Site 277, diversity and evenness decrease in the lower Oligocene (Supplementary Table 6).

Eocene sediments at Site 1172 consist of silty claystone with abundant diatoms. This sequence is overlain by a transitional unit in the ~~latest-uppermost~~ Eocene consisting of glauconitic siltstones, which indicate increased bottom-water currents ~~activity near the E-O boundary in the uppermost Eocene~~ (Kennett and Exon, 2004; Stickley et al., 2004). There is a sharp transition in the lowermost Oligocene to, a pelagic carbonate sequence consisting of nannofossil chalk ~~appears abruptly~~ (Exon et al., 2004). Diatoms are more abundant and of

inner neritic nature in the middle Eocene until ~408 mbsf (~39 Ma), where they become more oceanic and may indicate a change to a more outer neritic regime. Above ~376 mbsf (~38 Ma) the diatom assemblage indicates an inner to outer neritic regime (Röhl et al., 2004).

4.5 Trends in biogeographic affinities

~~Using the Eocene-Oligocene assemblage data collected at the four Southwest Pacific study sites, The radiolarian taxa assemblages at our five sites include 92 species or species groups that can be assigned to one of three were grouped according to their biogeographic affinity categories: high-latitude (5850 taxa), cosmopolitan (3938 taxa), and low-latitude (34 taxa) and unknown (31). (Table 1, Supplementary Table 12). Biogeographic affinities remain poorly known for the remaining 39 taxa encountered at DSDP sites 277, 280, 281 and 283, and for ~100 taxa at Site 1172 reported by Suzuki et al. (2009). Within the high-latitude group, several six taxa are bipolar (6) (*Artostrobus annulatus*, *Axoprunum bispiculum*, *Ceratocyrtis* spp., *Cycladophora cosma cosma*, *Pseudodictyophimus gracilipes* and *Spongopyle osculosa*), whereas 52-45 taxa are currently inferred only known to be endemic to the Southern Ocean (Table 1). Almost all species in the Litheliidae, Lophocyrtidae and Plagiacanthidae are high-latitude. The biogeographic affinity of *Lithelius minor* gr. is considered to be uncertain cosmopolitan, as some members may be confined to the high latitudes and others may be cosmopolitan. Because, but because this group is a major component very abundant in some assemblages, we consider it as part of the high latitude complex but separate it out in Figures 6 and 7. For Site 277, we also differentiate key high-latitude elements taxa within the three families noted above, namely *Larcopyle* spp., *Lophocyrtis longiventer* and *Lithomelissa* spp., and the actinommid *Axoprunum irregularis* (Figure 6).~~

At Site 277, taxa with high-latitude affinities are present from the base of the study section in the middle Eocene (Figure 6). The MECO is accompanied characterized by athen increase presence of in high-latitude taxa to of ~1923% (*Larcopyle* spp., *Lithelius minor* gr., *Lophocyrtis jacchia hapsis*, *L. longiventer*), but also the appearance of low-latitude species *Amphicraspedum murrayanum* and *A. proluxum* gr. (Sup to ~10% of total assemblage). *Lophocyrtis jacchia hapsis* is considered to be a high-latitude variant of *L. jacchia jacchia* and has a short stratigraphic range in the middle to late Eocene in the Southern Ocean (Sanfilippo and Caulet, 1998). In our study this taxon has a common appearance only during

Formatted: Font: Not Italic

the MECO and in the upper Eocene (Figure 6). In the middle of the PrOM event (~225 mbsf), diversity and high-latitude taxa increase (average of 28%) in conjunction with the appearance of *Lithomelissa* spp. and other high-latitude Lophocyrtiidae.

During the late Eocene warming event, high-latitude taxa decrease to ~13% at Site 277 and only rare occurrences of *Lithomelissa* spp. and high-latitude *Lophocyrtis* spp. are noted (Figure 6, Table 2). Late Eocene warming however coincides with the abundant occurrence of the low-latitude taxon *Thyrsoyrtis pinguisoides* (up to 20%) and the trace occurrence of *A. prolixum*. Cosmopolitan taxa are dominated by *Lychnocanium* spp. but general diversity also decreases within the warming event (Supplementary Table 1). The abundance of high-latitude taxa further increases at the start of the late Eocene, with increasing numbers of lophocyrtids, dominated by *L. longiventer* (Figure 6), and the radiolarian diversification during the PrOM event is marked by an increase *Lithomelissa* spp. *Amphycraspedum prolixum* gr. has a trace occurrence in the latest Eocene. After this event, high-latitude taxa increase to up to ~50% in the uppermost Eocene and lowermost Oligocene with the reappearance of all high-latitude taxa and an overall diversification (Figure 6, Table 2).

During the early-lower Oligocene, overall diversity declines and especially the delicate plagiacanthiids Plagiacanthiidae and lophocyrtids Lophocyrtiidae decrease in abundance. *Lithelius minor* gr. becomes dominant until ~144 mbsf. Above 144 mbsf, *Lithelius minor* gr., then this group decreases in abundance and high-latitude actinommids *Axoprunum bispiculum* and *A. irregularis* make up ~75% of the high-latitude assemblage (Figure 6, Supplementary Table 1).

At Sites 1172, and 283, high-latitude taxa are present in the middle and upper Eocene, although varying between ~3 and 40% of the assemblage for which biogeographic affinities have been established (Figure 7). comprising 20–30% of the assemblage at Site 1172 and ~40% at Site 283 (Figure 7). The MECO interval at Site 1172 (Core 1172D-45X; Bijl et al., 2010) corresponds to a decline minimum in high-latitude taxa, which is part of a longer minimum in high-latitude taxa from 430 to 410 mbsf, and an increase in cosmopolitan taxa. In the early-late Eocene (~38–37 Ma), high-latitude taxa increase at Site 1172, from ~30 to ~50%. The most profound increase in high-latitude taxa at Site 1172 occurs in the lower Oligocene (~50–80%) with an increase in abundance of *A. irregularis* to dominant levels, similar to Site 277. None of the low-latitude taxa found at the other sites are present at Site 1172.

At Site 283, high-latitude taxa are present from the middle Eocene and range between ~12 and 35%. *Lithelius minor* gr. is very abundant and varies between ~20–40% in all samples (Figure 7). We tentatively correlate the relatively high abundance in the low-latitude species *Theocyrtis tuberosa* (~9%) in the upper part of the studied section (87.75 mbsf) to the late Eocene warming event at Site 277. Sites 280 and 281 both have a higher proportion of high-latitude taxa in the lower upper Eocene to lower Oligocene than all other sites. High-latitude taxa at Site 281 range between 20–40 and 40–73% in the early-late lower upper Eocene at Site 281 and between ~50–73% in the lower Oligocene at Site 280, respectively (Figure 7). At Site 283 high-latitude taxa are more abundant ranging between 40 and 55%. However, this is mainly due to the high abundance of a single taxon, *Lithelius minor* gr. Several taxa that are present in the early-lower Oligocene at Site 280 are absent at Site 277, including *Lithomelissa challengerae*, *Larcopyle frakesi*, *Lithomelissa sakaii*, and *Antarctissa* spp. The percentage abundance of high-latitude taxa at Site 280 is between 45 and 55%, with *Lithelius minor* gr. of is also high at sites 280 and 281, ranging between ~20–40–20–40%. *Amphycraspedum prolixum* gr. has a trace occurrence at ~103 mbsf at Site 280.

5 Discussion

5.1 Comparison with geochemical temperature proxies

The radiolarian assemblages documented at Sites 277 and 1172 within the MECO interval lack typical tropical taxa such as *Thyrsocyrtis* spp. or *Podocyrtis* spp. (e.g. Kamikuri et al., 2012), and Taxa with the low-latitude affinities taxa, such as *Amphycraspedum* *Amphycraspedum murrayanum* and *A. prolixum* gr., account for only 5% of the total assemblage at Site 277 and are absent at Site 1172. The persistence of high-latitude taxa and the variety of cosmopolitan species at both sites suggests a warm-temperate climate of (15–20°C, Nelson and Cooke, 2001), in contrast to geochemical proxies suggesting a tropical climate (>25°C) for the MECO at Site 1172 (Bijl et al., 2010) and ~27°C for the latest Eocene at Site 277 (Liu et al., 2009). The sea surface temperature estimates were derived from organic proxies (TEX₈₆ and U^{K'}₃₇) and may be biased towards summer temperatures (Liu et al., 2009; Hollis et al., 2012). Although the interval of peak warmth may not be preserved in the MECO at Site 277, the relatively low abundance of Tropical radiolarian taxa

within the PETM and early Eocene climatic optimum in the Southwest Pacific has also been previously noted by Hollis (2006; Hollis et al., 2014).

5.2 Nature of the Antarctic assemblage

High-latitude taxa existed from at least the middle Eocene at sites 277, 283 and 1172. Many taxa that are present from the earliest late Eocene (~38 Ma) at ~~S~~ sites 281 and 283 appear later at Site 277 ~~(~37–36 Ma)~~, during the PrOM event ~~(~37 Ma), coinciding. This appearance~~ ~~coincides~~ with an increase in radiolarian abundance, diversity and preservation. A comparison of all high-latitude groups is shown in Table 2. We assigned all *Lithomelissa* spp. and *Larcopyle* spp. to the high-latitude group as they are more abundant at higher-latitude sites. ~~Although we assigned a cosmopolitan affinity to~~ ~~The ecological and biogeographic~~ ~~affinity of~~ *Lithelius minor* gr., ~~the paleoecology of this group~~ is not yet fully understood, ~~as it: This group has a cosmopolitan distribution but~~ tends to be most abundant at high-latitude sites. The sudden appearance of *Lithomelissa* spp. ~~and~~, other high-latitude taxa and diatoms at Site 277 indicates the expansion of high-latitude water masses across the southern Campbell Plateau in two phases: first during the PrOM event and again after the late Eocene warming event when a second diversification and influx of high-latitude taxa is observed.

5.3 High-latitude cooling and eutrophication during the PrOM event

5.3.1 Diagenesis

One ~~possibility possible explanation is that for~~ the pronounced increase in radiolarian abundance and diversity ~~observed in the Late upper Eocene of at~~ Site 277 is that these trends are an artefact of biogenic opal diagenesis. Chert nodules are recorded throughout the upper Paleocene-to-middle Eocene section of the cored sequence at Site 277, with a transition between chert-bearing nannofossil chalk and overlying nannofossil ~~ooze recorded~~ at 246 mbsf ~~(early late lower upper Eocene)~~ (Kennett et al., 1975). The presence of chert combined with the generally poorer preservation of radiolarians in the lower Paleogene interval indicates some degree of diagenesis, which is also reflected in the range-through taxic richness analysis. However, the first major radiolarian turnover event occurs ~20 m above the lithological transition ~~from chert-bearing nannofossil chalk to within the succession of~~ nannofossil oozes, which implies that the event represents a real increase in radiolarian and diatom abundance and not an artefact of ~~preservation~~ diagenesis. No lithological changes are

present at that levels which could explain the observed diversity decrease during the late Eocene warming event and the increase in diversity thereafter.

5.3.2 Climate cooling

The long-term cooling trend through the middle and late Eocene, which was interrupted by the short-lived MECO warming event, ~~cannot~~ does not explain the sudden radiolarian diversification in the late Eocene at Site 277. If gradual, long-term cooling was the driver of the expansion of high-latitude taxa, a progressive increase in such taxa would be expected over a longer time period. A gradual increase of high-latitude taxa is observed at Site 1172 from the middle Eocene but not at Site 277. Instead, the short-lived PrOM event ~~was likely~~ appears to have been the trigger for the ~~sudden-northward~~ expansion of high-latitude taxa ~~towards the north~~ onto the Campbell Plateau. Whether ~~that-this~~ event was caused by an ~~abrupt-sudden drop decline~~ in atmospheric CO₂ concentrations or was related to the opening of the Tasmanian Gateway, which may have been open to surface circulation in early middle Eocene (Bijl et al., 2013), cannot be determined. Furthermore, astronomically induced changes also may have ~~to be considered~~ had a role. ~~Reconstructions from~~ Laskar et al. (2004) ~~calculated~~ show that nodes in the amplitude modulation of eccentricity and obliquity ~~are present~~ at ~37 Ma ~~and~~ Additionally, Röhl et al. (2004) found evidence at Site 1172 for the increasing dominance of the 100 kyr eccentricity cycle at ~37 Ma. Although there are nodes in amplitude modulation throughout the Eocene (Laskar et al, 2004), it is ~~likely that only the possible that a~~ combination of ~~all parameters~~ these phenomena (e.g., a decrease in atmospheric CO₂ ~~drop~~, gateway opening and nodes in amplitude modulation) ~~crossed a certain threshold for~~ caused a cooling event. The amplitude modulation of obliquity, in particular, has been linked to climatic cooling in the Oligocene (Pälike et al., 2006).

The PrOM event at ~37 Ma may have been associated with the formation of small Antarctic ice sheets (Scher et al., 2014), which ~~in turn would have resulted in~~ may have caused an intensification of currents in the Southern Ocean. Funakawa and Nishi (2008) reported a marked increase in radiolarian taxa with Antarctic faunal affinities at ODP Site 689 (Maud Rise, southern Atlantic) in the earliest late Eocene (~38.6–36.9 Ma; Chron C17), which they interpreted to signify the northward expansion of the polar front that may be related to the PrOM. Several radiolarian turnover events are recorded from the South Atlantic (Maud Rise) by Funakawa and Nishi (2008) during the late Eocene to early Oligocene. At ~38.5 Ma they

identified a shift from subantarctic to Antarctic bioprovinces with an increase in Antarctic taxa. At ~36.3 Ma a subsequent decrease in Antarctic taxa, spanning Chrons 16 and 15 (~37–35 Ma), was observed and was related to the late Eocene warming event of (Bohaty and Zachos, 2003). These cooling and warming events appear to have caused longer-lived changes in radiolarian faunal assemblages than those observed at Site 277, lasting 1.7 and 2.0 Ma, respectively. This may reflect specific differences in the oceanographic settings of the two sites. Although the Both events were explained by the northward and southward shift of a proto Antarctic Polar Front, respectively, however, the first event is not identical with the PrOM event. late Eocene warming event appears to be short-lived at Site 277, it may have spanned a longer interval of time elsewhere in the Southwest Pacific. Incursions of warm-water foraminifera, including the low-latitude genus *Hantkenina*, are known to have occurred in the middle late Eocene (late Kaiatan-early Runangan) in sedimentary basins of southern New Zealand (Hornibrook et al., 1989; Hornibrook, 1992).

5.3.3 Radiolarian biogeographic reconstruction

During the middle Eocene, high-latitude radiolarian taxa were present at sites 277, 283, and 1172 (Figure 7). The short-lived increase in abundance, diversity and the influx of low-latitude radiolarian ~~*Amphycraspedum*~~ *Amphicraspedum murrayanum* and *A. prolixum* gr. during the MECO at Site 277 and a high percentage of cosmopolitan taxa at Site 1172 during the late middle Eocene suggest moderately warm temperatures at both sites, which may have been the result of a slightly stronger influence of an East Australian Current (EAC) (Figure 8A). However, radiolarians and diatoms were abundant only at Site 1172 during the middle Eocene, which suggests a higher productivity region, perhaps a consequence of local of upwelling. The Tasmanian Gateway was open to a shallow westward flowing Antarctic Slope Current (ASC), driven by the polar easterlies (Bijl et al., 2013; Scher et al. 2015).

During the middle to onset of the PrOM event in the early late Eocene (~39.38–38.37 Ma, Figure 8B), the abundance of high-latitude taxa increases increased at Site sites 1172 and 277. Additionally, Sites sites 281 and 283 show were characterized by high radiolarian abundance, with an average of ~25–61 to and almost 50–27% high-latitude taxa, respectively. The region of high-productivity is expanding expanded in this time, with the southernmost Site 281 sites having the highest D/R ratio in the interval ~39–38 Ma (Figure 8B). The region might have experienced an intensification of the Ross gyre, extending the region of high

productivity onto the Campbell Plateau and creating a Subtropical Front (STF) (Nelson and Cooke, 2001) (Figure 8B). This could have resulted from further gateway opening and an intensified cold water proto-Ross gyre. Radiolarian abundance is still low at Site 277.

~~In the late Eocene~~ During the late Eocene warming event (~37–35–36 Ma, Figure 8C), radiolarian ~~diversity abruptly diversified~~ ~~decreased abruptly and increase in abundance~~ at Site 277, together with a decrease in ~~high-latitude taxa~~ ~~appear~~ (*Lithomelissa* spp., *Larcopyle* spp., Lophocyrtiidae, Table 2) and diatoms, and the appearance of ~~together with diatoms~~, low-latitude taxa at sites 283 and 277, ~~resulting from cooling and eutrophication at Site 277~~. High-latitude taxa increase at Site 1172 from ~36.5 Ma (Figure 7), whereas Site 281 contains a late Eocene hiatus, implying an increase in the strength of bottom water currents across the Tasmanian Gateway. We suggest that these changes were associated with a southward shift of the EAC that pushed the high-productivity zone of the STF towards the south, explaining the low radiolarian abundance and drop in diversity at Site 277. There is little evidence that the large Tasman Current as proposed by Huber et al. (2004) and Bijl et al. (2010) existed in the middle and late Eocene. Instead, our data suggest Site 277 was positioned at the northernmost limit of the influence of the Ross Gyre and the southernmost site of the influence of warm water delivered by the EAC. ~~Site 281 contains a late Eocene hiatus, implying that increasing bottom water currents were established across the Tasmanian Gateway.~~

During the ~~early Oligocene~~ latest Eocene-earliest Oligocene interval (~33–35–32 Ma, Figure 8D), Site 277 experienced a second siliceous plankton bloom, associated with high radiolarian and diatom abundance and the reappearance of high-latitude taxa (Table 2). This suggests that latest Eocene cooling led to the expansion of the Ross Gyre to encroach on Campbell Plateau (Figure 8D). At the same time and perhaps reflecting strengthening of northward and westward flowing bottom currents, the area of non-deposition widened across the Tasmanian Gateway over sites 281, 283 and 1172. During the earliest Oligocene, the abundance of radiolarians and diatoms at ~~suggesting the fully open gateway and deep water connection between ocean basins was established~~. Only Site 280 has a radiolarian and diatom-rich record in the early Oligocene ~~indicating suggests~~ a high primary productivity region. This may have been a consequence of intensified upwelling associated with the ASC in conjunction with deepening in this sub-basin. About 50% of the radiolarian fauna are high-

latitude taxa at that site. Site 277 also shows high radiolarian abundance and increasing high-latitude portion (~40%) at ~33 Ma (Figure 8D). The

In contrast, diversity, however, declines at Site 277 in the early Oligocene (Figure 8E) and diatoms are rare or absent become scarce. The radiolarian fauna becomes dominated by *Lithelius minor* gr. and Actinommidae and many other high-latitude taxa disappear (e.g. *Lithomelissa* spp., Table 2). This may be related to the development of the ACC. The ACC is inferred to have developed at ~30 Ma as the Tasmanian Gateway became fully open (Carter et al., 2004) and its northward expansion brought it in line with the westerly wind belt (Scher et al., 2015). This resulted in the zone of non-deposition extending over Site 280 as it moved into the path of the ACC. At Site 277, the radiolarian fauna is dominated by the high-latitude species *Axoprunum irregularis*, which is also dominant at Site 1172. Thus, the general low diversity of radiolarians and the scarcity of diatoms at Site 277 This may indicate suggests the establishment of a cold-water nutrient-depleted environment, similar to the modern setting (Hollis and Neil, 2005). The development of the ACC restricted the northward extent of Ross Gyre and served to establish the, with a proto-Subantarctic Front being established to on the southern margin of the Campbell Plateau (Carter et al., 2004).

6 Conclusions

Middle Eocene to early Oligocene radiolarian assemblages from DSDP sites 277, 280, 281, 283 and ODP Site 1172 were examined to investigate the relative influence of low- and high-latitude water masses in the southern Southwest Pacific Ocean as global climate cooled and ice sheets expanded in Antarctica to identify the distribution of Antarctic assemblages in the Southwest Pacific. In contrast to temperature reconstructions based on geochemical proxies that indicate subtropical-tropical temperatures at high-latitudes during the middle and late Eocene (Liu et al., 2009; Bijl et al., 2010), Eocene radiolarian assemblages in this region lack significant numbers of low-latitude warm-water taxa. Furthermore, we show that many high-latitude and taxa endemic to the Antarctic are already present in the middle Eocene. The MECO event, although truncated by poor recovery, has been identified at Site 277 within from foraminiferal $\delta^{18}\text{O}$ oxygen isotope records, and is associated with a short-lived incursion of two taxa with low-latitude taxa affinities, *Amphycraspedum* *Amphicraspedum* *prolixum* gr. and *Amphycraspedum* *A. murrayanum*, in low numbers. The absence of definitive tropical

Tropical taxa suggests warm temperate rather than tropical conditions during this short-lived event. ~~However, the peak warming interval is likely missing due to poor core recovery.~~

Radiolarians are very abundant and well preserved at high-latitude sites 281, 283 and 1172 during the early late Eocene and at Site 280 during the early Oligocene. For taxa with identified biogeographic affinities, those with high-latitude affinities comprise ~60% at sites 280 and 281 and ~30% at sites 283 and 1172 ~~with about 30–50% of the assemblage consisting of high-latitude taxa.~~ During the early late Eocene (~37 Ma), a positive ~~excursion shift~~ in foraminiferal $\delta^{18}\text{O}$ values at Site 277 marks the onset of the PrOM event. A pronounced increase in diversity, abundance and preservation of radiolarians occurs in conjunction with this event at Site 277 in addition to a ~~It is also accompanied by a pronounced marked increase in the abundance of diatoms~~ diatom abundance. Many high-latitude taxa that are very abundant at ~~S~~ites 281 and 283 in the late middle Eocene and early late Eocene become abundant or have their LOs at Site 277 at ~37 Ma, ~~respectively~~ including: *Lithelius minor* gr., *Larcopyle hayesi*, *L. polyacantha*, *Spongopyle osculosa*, *Lithomelissa sphaerocephalis*, *L. gelasinus*, *L. ehrenbergi*, *Ceratocyrtis* spp., *Dictyophimus* aff. *archipilum*, *Lamprocyclas particollis*, and Antarctic morphotypes of *Aphetocyrtis gnomabax*, *A. rossi*, *Lophocyrtis aspera*, *L. kraspera* and *L. longiventer*. This northward extension of high-latitude taxa onto the Campbell Plateau appears to have been triggered by cooling during the PrOM event, which ~~is inferred to have been~~ may have been associated with a short-lived ~~expansion~~ development of ~~an~~the Antarctic ice sheet.

A late Eocene warming event at ~36 Ma is accompanied by a decrease in radiolarian diversity, high-latitude taxa and low diatom abundance at Site 277. Two low-latitude taxa, Theocyrtis tuberosa and Thyrsocyrtis pinguisoides, make short-lived incursions into the Southwest Pacific at this time. After this event, radiolarian diversity increases again with the reappearance of high-latitude taxa and abundant diatoms at Site 277. Through the EOT, radiolarians remain abundant at Site 277, but decline in diversity ~~decrease in abundance and diversity at Site 277. Delicate forms~~ Most nassellarian taxa such as within the Plagiacanthidae and Lophocyrtiidae decline, whereas *Lithelius minor* gr. and Actinommidae ~~became~~ become dominant. Together with the ~~The disappearance~~ scarcity of diatoms, we infer ~~indicates~~ that conditions over the Campbell Plateau became nutrient-depleted as a consequence of the development of the ACC. The establishment of the ~~We infer that the Tasmanian Gateway was fully open by the earliest Oligocene and a strong circumpolar current~~ ACC at around

~~30 Ma is inferred to have caused~~~~was established causing~~ widespread non-deposition in the Southwest Pacific ~~and restricted the northward flow of Ross Gyre. At the same time, a proto-Subantarctic Front developed supplying nutrient depleted Subantarctic waters onto the Campbell Plateau resulting in a decline in radiolarian and diatom productivity.~~

Acknowledgements

This study ~~has~~ used bulk material and reference slides stored in the DSDP/ODP Micropaleontology Reference Centre, which is located at ~~the Institute of Geological and Nuclear~~GNS Sciences, Lower Hutt, New Zealand. ~~We greatly appreciate the reviews of David Lazarus and an anonymous referee that provided helpful comments in improving our manuscript. We thank Noritoshi Suzuki (Tohoku University, Japan) for providing unpublished radiolarian data for ODP Site 1172.~~ We acknowledge the technical support of ~~Hannu Seebeck~~Sonja Bermudez (GNS Science), James Crampton (GNS Science) and Johan Renaudie (Museum für Naturkunde, Berlin) and editorial handling by Gerald Dickens.~~in generating the paleogeographic maps.~~ This project is funded by the New Zealand Marsden Fund (Contract GNS1201).

References

- Barron, J. A., Stickley, C. E., and Bukry, D.: Paleooceanographic, and paleoclimatic constraints on the global Eocene diatom and silicoflagellate record, *Palaeogeogr. Palaeoclimatol. Palaeoecol.*, 422, 85-100, [doi:10.1016/j.palaeo.2015.01.015](https://doi.org/10.1016/j.palaeo.2015.01.015), 2015.
- Bijl, P. K., Houben, A. J., Schouten, S., Bohaty, S. M., Sluijs, A., Reichert, G.-J., Damsté, J. S. S., and Brinkhuis, H.: Transient Middle Eocene atmospheric CO₂ and temperature variations, *Science*, 330, 819-821, 2010.
- Bijl, P. K., Bendle, J. A., Bohaty, S. M., Pross, J., Schouten, S., Tauxe, L., Stickley, C. E., McKay, R. M., Röhl, U., and Olney, M.: Eocene cooling linked to early flow across the Tasmanian Gateway, *Proc. Natl. Acad. Sci. U.S.A.*, 110, 9645-9650, 2013.
- Bird, P.: An updated digital model of plate boundaries, *Geochem. Geophys. Geosyst.*, 4(3), 1027, doi:10.1029/2001GC000252, 2003.

Bohaty, S. M., and Zachos, J. C.: Significant Southern Ocean warming event in the late middle Eocene, *Geology*, 31, 1017-1020, [doi: 10.1130/G19800.1](https://doi.org/10.1130/G19800.1), 2003.

Bohaty, S. M., Zachos, J. C., Florindo, F., and Delaney, M. L.: Coupled greenhouse warming and deep-sea acidification in the middle Eocene, *Paleoceanography*, 24, PA2207, [doi:10.1029/2008PA001676](https://doi.org/10.1029/2008PA001676), 2009.

Bohaty, S. M., Zachos, J. C., and Delaney, M. L.: Foraminiferal Mg/Ca evidence for Southern Ocean cooling across the Eocene–Oligocene transition, *Earth and Planetary Science Letters*, 317, 251-261, [doi:10.1016/j.epsl.2011.11.037](https://doi.org/10.1016/j.epsl.2011.11.037), 2012.

[Boyden, J. A., Müller, R. D., Gurnis, M., Torsvik, T. H., Clark, J. A., Turner, M., Ivey-Law, H., Watson, R. J., and Cannon, J. S.: Next-generation plate-tectonic reconstructions using GPlates, *Geoinformatics: cyberinfrastructure for the solid earth sciences*, 95-114, 2011. \[<http://www.gplates.org/index.html>; download on 25-09-2015\]](#)

[Cande, S. C., and Stock, J. M.: Pacific—Antarctic—Australia motion and the formation of the Macquarie Plate, *Geophys. J. Int.*, 157, 399-414, 2004.](#)

[Carter, L., Carter, R., and McCave, I.: Evolution of the sedimentary system beneath the deep Pacific inflow off eastern New Zealand, *Marine Geology*, 205, 9-27, 2004.](#)

Casey, R. E.: Radiolaria, in: *Fossil Prokaryotes and Protists*, edited by: Lipps, J. H., Blackwell Scientific Publications, Oxford/London, UK, 249-284, 1993.

Caulet, J. P.: Radiolarians from the Kerguelen Plateau, Leg 119, in: Barron, J.A., Larsen, B. et al., *Proceedings ODP, Scientific Results*, 119, College Station, TX (Ocean Drilling Program), 513-546, 1991.

Chen, P. H.: Antarctic Radiolaria, in: Hayes, D.E., Frakes, L.A., et al., *Initial Reports of the Deep Sea Drilling Project*, Vol. 28, U.S. Government Printing Office, Washington, D.C., 437-513, 1975.

[Coxall, H. K., Wilson, P. A., Pälike, H., Lear, C. H., & Backman, J.: Rapid stepwise onset of Antarctic glaciation and deeper calcite compensation in the Pacific Ocean. *Nature*, 433\(7021\), 53-57, 2005.](#)

[Croon, M. B., Cande, S. C., and Stock, J. M.: Revised Pacific-Antarctic plate motions and geophysics of the Menard Fracture Zone, *Geochem. Geophys. Geosyst.*, 9, Q07001, \[doi:10.1029/2008GC002019\]\(https://doi.org/10.1029/2008GC002019\), 2008.](#)

- 1 Crouch, E. M., and Hollis, C. J.: Paleogene palynomorph and radiolarian biostratigraphy of
2 DSDP Leg 29, sites 280 and 281 South Tasman Rise, Institute of Geological and Nuclear
3 Sciences science report 96/19, 46p., 1996.
- 4 Diester-Haass, L., and Zahn, R.: Eocene-Oligocene transition in the Southern Ocean: History
5 of water mass circulation and biological productivity, *Geology*, 24, 163-166, 1996.
- 6 Diester-Haass, L., Robert, C., and Chamley, H.: The Eocene-Oligocene preglacial-glacial
7 transition in the Atlantic sector of the Southern Ocean (ODP Site 690), *Mar. Geol.*, 131, 123-
8 149, 1996.
- 9 Edwards, A. R., and Perch-Nielsen, K.: Calcareous nannofossils from the southern southwest
10 Pacific, Deep Sea Drilling Project, Leg 29, in: Kennett, J. P., Houtz, R. E., et al., Initial
11 Reports of the Deep Sea Drilling Project, Vol. 29, Washington, DC, US Government Printing
12 Office, 469-539, 1975.
- 13 Exon, N. F., Kennett, J. P., and Malone, M. J.: Leg 189 synthesis: Cretaceous-Holocene
14 history of the Tasmanian gateway, in: Proceedings ODP, Scientific Results, 2004.
- 15 Florindo, F., and Roberts, A. P.: Eocene-Oligocene magnetobiochronology of ODP Sites 689
16 and 690, Maud Rise, Weddell Sea, Antarctica, *Geol. Soc. Am. Bull.*, 117, 46-66, 2005.
- 17 Funakawa, S., and Nishi, H.: Late middle Eocene to late Oligocene radiolarian
18 biostratigraphy in the Southern Ocean (Maud Rise, ODP Leg 113, Site 689), *Mar.*
19 *Micropaleontol.*, 54, 213-247, 2005.
- 20 Funakawa, S., and Nishi, H.: Radiolarian faunal changes during the Eocene-Oligocene
21 transition in the Southern Ocean (Maud Rise, ODP Leg 113, Site 689) and its significance in
22 paleoceanographic change, *Micropaleontology*, 54, 15-26, 2008.
- 23 Funakawa, S., Nishi, H., Moore, T. C., and Nigrini, C. A.: Radiolarian faunal turnover and
24 paleoceanographic change around Eocene/Oligocene boundary in the central equatorial
25 Pacific, ODP Leg 199, Holes 1218A, 1219A, and 1220A, *Palaeogeogr. Palaeoclimatol.*
26 *Palaeoecol.*, 230, 183-203, 2006.
- 27 [Gradstein, F., Ogg, J., Schmitz, M., and Ogg, G.: The geologic time scale 2012, vol. 2,](#)
28 [Elsevier New York, 2012.](#)

Granot, R., Cande, S., Stock, J., and Damaske, D.: Revised Eocene-Oligocene kinematics for the West Antarctic rift system, *Geophys. Res. Lett.*, 40, 279-284, doi: [10.1029/2012GL054181](https://doi.org/10.1029/2012GL054181), 2013.

Hammer, Ø., Harper, D., and Ryan, P.: Past: Paleontological Statistics Software Package for education and data analysis. *Paleontología Electrónica* 4: 1-9, http://palaeo-electronica.org/2001_1/past/issue1_01.html, 2001. [\[download of version 3.17 on 24-07-2015, http://folk.uio.no/ohammer/past/\]](http://folk.uio.no/ohammer/past/)

Hollis, C. J.: Biostratigraphy and paleoceanographic significance of Paleocene radiolarians from offshore eastern New Zealand, *Mar. Micropaleontol.*, 46, 265-316, 2002.

~~Hollis, C. J.: Radiolarian faunal turnover through the Paleocene-eocene transition, Mead Stream, New Zealand, in: Radiolaria, Springer, 79-99, 2006.~~

[Hollis, C. J.: Radiolarian faunal change across the Paleocene-Eocene boundary at Mead Stream, New Zealand, *Eclogae Geol. Helv.*, 99, S79-S99, 2006.](#)

[Hollis, C., and Neil, H.: Sedimentary record of radiolarian biogeography, offshore eastern New Zealand, *New Zeal. J. Mar. Fresh.*, 39, 165-192, 2005.](#)

Hollis, C. J., Waghorn, D. B., Strong, C. P., and Crouch, E. M.: Integrated Paleogene Biostratigraphy of DSDP Site 277 (Leg 29): Foraminifera, Calcareous Nannofossils, Radiolaria, and Palynomorphs, Institute of Geological & Nuclear Sciences Limited, 1997.

[Hollis, C. J., Dickens, G. R., Field, B. D., Jones, C. M., and Percy Strong, C.: The Paleocene–Eocene transition at Mead Stream, New Zealand: a southern Pacific record of early Cenozoic global change, *Palaeogeogr. Palaeoclimatol. Palaeoecol.*, 215, 313-343, 2005.](#)

Hollis, C. J., Taylor, K. W. R., Handley, L., Pancost, R. D., Huber, M., Creech, J. B., Hines, B. R., Crouch, E. M., Morgans, H. E. G., Crampton, J. S., Gibbs, S., Pearson, P. N., and Zachos, J. C.: Early Paleogene temperature history of the Southwest Pacific Ocean: Reconciling proxies and models, *Earth Planet. Sci. Lett.*, 349, 53-66, DOI [10.1016/j.epsl.2012.06.024](https://doi.org/10.1016/j.epsl.2012.06.024), 2012.

[Hollis, C. J., Pascher, K. M., Hines, B. R., Littler, K., Kulhanek, D. K., Strong, C. P., Zachos, J. C., Eggins, S. M. and Philips, A.: Was the Early Eocene ocean unbearably warm or are the proxies unbelievably wrong? *Rendiconti Online* 31, 109-110, 2014.](#)

- 1 [Hornibrook, N. d. B.: New Zealand Cenozoic marine paleoclimates: a review based on the](#)
- 2 [distribution of some shallow water and terrestrial biota, Pacific Neogene: environment,](#)
- 3 [evolution, and events. University of Tokyo Press, Tokyo, 83-106, 1992.](#)
- 4 Hornibrook, N. de B., Brazier, R. C., and Strong, C. P.: Manual of New Zealand Permian to
- 5 Pleistocene foraminiferal biostratigraphy, Paleontological bulletin/New Zealand Geological
- 6 Survey, 56, 1-175, 1989.
- 7 Houben, A. J., Bijl, P. K., Pross, J., Bohaty, S. M., Passchier, S., Stickley, C. E., Röhl, U.,
- 8 Sugisaki, S., Tauxe, L., and van de Flierdt, T.: Reorganization of Southern Ocean Plankton
- 9 Ecosystem at the Onset of Antarctic Glaciation, Science, 340, 341-344, 2013.
- 10 Huber, M., and Sloan, L. C.: Heat transport, deep waters, and thermal gradients: Coupled
- 11 simulation of an Eocene greenhouse climate, Geophys. Res. Lett., 28, 3481-3484, 2001.
- 12 [Huber, M., Sloan, L. C., and Shellito, C.: Early Paleogene oceans and climate: A fully](#)
- 13 [coupled modeling approach using the NCAR CCSM, Geological Society of America Special](#)
- 14 [Papers, 369, 25-47, 2003.](#)
- 15 Huber, M., Brinkhuis, H., Stickley, C. E., Döös, K., Sluijs, A., Warnaar, J., Schellenberg, S.
- 16 A., and Williams, G. L.: Eocene circulation of the Southern Ocean: Was Antarctica kept
- 17 warm by subtropical waters?, Paleoclimatology, 19, PA4026, doi:10.1029/2004PA001014,
- 18 2004.
- 19 Jenkins, D. G.: Cenozoic planktic foraminiferal biostratigraphy of the southwestern Pacific
- 20 and Tasman Sea - DSDP Leg 29, in: Kennett, J.P., Houtz, R.E. et al., Initial Reports of the
- 21 Deep Sea Drilling Project, Vol. 29, U.S. Government Printing Office, Washington, D.C. ,
- 22 449-467, 1975.
- 23 Kamikuri, S.-i., Moore, T. C., Lyle, M., Ogane, K., and Suzuki, N.: Early and Middle Eocene
- 24 radiolarian assemblages in the eastern equatorial Pacific Ocean (IODP Leg 320 Site U1331):
- 25 Faunal changes and implications for paleoclimatology, Mar. Micropaleontol., 98, 1-13,
- 26 doi:10.1016/j.marmicro.2012.09.004, 2013.
- 27 [Katz, M. E., Miller, K. G., Wright, J. D., Wade, B. S., Browning, J. V., Cramer, B. S.,](#)
- 28 [Rosenthal, Y.: Stepwise transition from the Eocene greenhouse to the Oligocene icehouse.](#)
- 29 [Nature Geoscience, 1\(5\), 329-334, 2008.](#)

1 Keigwin, L.: Palaeoceanographic change in the Pacific at the Eocene-Oligocene boundary,
2 Nature, 287, 722-725, 1980.

3 [Keller, W.R.: Cenozoic plate tectonic reconstructions and plate boundary processes in the](#)
4 [Southwest Pacific. Unpub. PhD Thesis: California Institute of Technology. Pasadena, 2003.](#)

5 Kennett, J. P.: Cenozoic evolution of Antarctic glaciation, the circum-Antarctic Ocean, and
6 their impact on global paleoceanography, J. Geophys. Res., 82, 3843-3860, 1977.

7 Kennett, J. P.: The development of planktonic biogeography in the Southern Ocean during
8 the Cenozoic, Mar. Micropaleontol., 3, 301-345, 1978.

9 Kennett, J. P., and Exon, N. F.: Paleoceanographic evolution of the Tasmanian Seaway and
10 its climatic implications, in: The Cenozoic Southern Ocean: Tectonics, Sedimentation, and
11 Climate Change Between Australia and Antarctica, Geoph. Monog. Series 151, 345-367,
12 2004.

13 Kennett, J. P., Houtz, R. E., Andrews, P. B., Edwards, A. R., Gostin, V. A., Hajós, M.,
14 Hampton, M., Jenkins, D. G., Margolis, S., Owenshine, T., and Perch-Nielsen, K.: Initial
15 Reports of the Deep Sea Drilling Project, Vol. 29, U.S. Government Printing Office,
16 Washington, D.C., 1975.

17 Laskar, J., Robutel, P., Joutel, F., Gastineau, M., Correia, A., and Levrard, B.: A long-term
18 numerical solution for the insolation quantities of the Earth, Astron. Astrophys., 428, 261-
19 285, 2004.

20 Lazarus, D., and Caulet, J. P.: Cenozoic Southern Ocean reconstructions from
21 sedimentologic, radiolarian, and other microfossil data, Antarct. Res. Ser., 60, 145-174, 1993.

22 [Lazarus, D.: Neptune: A marine micropaleontology database, Math. Geol., 26, 817-832,](#)
23 [10.1007/BF02083119, 1994. \[last access: 21-08- 2015\]](#)

24 Lazarus, D., Hollis, C., and Apel, M.: Patterns of opal and radiolarian change in the Antarctic
25 mid-Paleogene: Clues to the origin of the Southern Ocean, Micropaleontology, 54, 41-48,
26 2008.

27 Liu, Z., Pagani, M., Zinniker, D., DeConto, R., Huber, M., Brinkhuis, H., Shah, S. R., Leckie,
28 R. M., and Pearson, A.: Global cooling during the Eocene-Oligocene climate transition,
29 Science, 323, 1187-1190, 2009.

- 1 [Liu, J., Aitchison, J. C., and Ali, J. R.: Upper Paleocene radiolarians from DSDP Sites 549](#)
2 [and 550, Goban Spur, NE Atlantic, *Palaeoworld*, 20, 218-231, 2011.](#)
- 3 Lunt, D. J., Dunkley Jones, T., Heinemann, M., Huber, M., LeGrande, A., Winguth, A.,
4 Loftson, C., Marotzke, J., Roberts, C., and Tindall, J.: A model–data comparison for a multi-
5 model ensemble of early Eocene atmosphere–ocean simulations: EoMIP, *Clim. Past*, 8, 1717-
6 1736, 2012.
- 7 Matthews, K. J., Williams, S. E., Whittaker, J. M., Müller, R. D., Seton, M., and Clarke, G.
8 L.: Geologic and kinematic constraints on Late Cretaceous to mid Eocene plate boundaries in
9 the southwest Pacific, *Earth Sci. Rev.*, 140, 72-107, 2015.
- 10 [Morgans, H. E. G.: Late Paleocene to Middle Eocene foraminiferal biostratigraphy of the](#)
11 [Hampden Beach section, eastern South Island, New Zealand. *New Zeal. J. Geol. Geop.*, 52,](#)
12 [273-320, 2009.](#)
- 13 Nelson, C. S., and Cooke, P. J.: History of oceanic front development in the New Zealand
14 sector of the Southern Ocean during the Cenozoic—a synthesis, *New Zeal. J. Geol. Geop.*,
15 44, 535-553, 2001.
- 16 O'Connor, B.: Stratigraphic and geographic distribution of Eocene Miocene Radiolaria from
17 the southwest Pacific, *Micropaleontology*, 46, 189-228, 2000.
- 18 Pälike, H., Shackleton, N. J., and Röhl, U.: Astronomical forcing in Late Eocene marine
19 sediments, *Earth Planet. Sci. Lett.*, 193, 589-602, 2001.
- 20 [Pälike, H., Frazier, J., & Zachos, J. C.: Extended orbitally forced palaeoclimatic records from](#)
21 [the equatorial Atlantic Ceara Rise. *Quaternary Sci. Rev.*, 25\(23\), 3138-3149, 2006.](#)
- 22 [Pearson, P. N., Ditchfield, P. W., Singano, J., Harcourt-Brown, K. G., Nicholas, C. J., Olsson,](#)
23 [R. K., Shackleton, N. J., and Hall, M. A.: Warm tropical sea surface temperatures in the Late](#)
24 [Cretaceous and Eocene epochs, *Nature*, 413, 481-487, 2001.](#)
- 25 Petrushevskaya, M. G.: Cenozoic radiolarians of the Antarctic, Leg 29, DSDP, in: Initial
26 Reports of the Deep Sea Drilling Project, edited by: Kennett, J. P., Houtz, R. E., et al., US
27 Government Printing Office, Washington, DC, vol. 29, 541-675, 1975.
- 28 Raine, J. I., Beu, A. G., Boyes, A. F., Campbell, H. J., Cooper, R. A., Crampton, J. S.,
29 Crundwell, M. P., Hollis, C. J., and Morgans, H. E. G.: Revised calibration of the New

1 Zealand Geological Timescale : NZGT2015/1, Lower Hutt, N.Z.: GNS Science. GNS
2 Science report 2012/39. 53 p, 2015.

3 Röhl, U., Brinkhuis, H., Stickley, C. E., Fuller, M., Schellenberg, S. A., Wefer, G., and
4 Williams, G. L.: Sea level and astronomically induced environmental changes in middle and
5 late Eocene sediments from the East Tasman Plateau, in: Exon, N.F., Kennett, J.P., and
6 Malone, M.J. (Eds.), The Cenozoic Southern Ocean: tectonics, sedimentation, and climate
7 change between Australia and Antarctica. Am. ~~geophys~~Geophys. Union, Geophys. Monogr.,
8 151, 127-151, 2004.

9 Sanfilippo, A., and Caulet, J. P.: Taxonomy and evolution of Paleogene Antarctic and Tropical
10 Lophocyrtid radiolarians, *Micropaleontology*, 44, 1-43, 1998.

11 Sanfilippo, A., Westberg-Smith, M. J., and Riedel, W. R.: Cenozoic radiolaria, in: *Plankton*
12 *stratigraphy: Volume 2, Radiolaria, Diatoms, Silicoflagellates, Dinoflagellates and*
13 *Ichthyoliths*, edited by: Bolli, H. M., Saunders, J. B., and Perch-Nielsen, K., 631-712, 1985.

14 Scher, H. D., Bohaty, S. M., Smith, B. W., and Munn, G. H.: Isotopic interrogation of a
15 suspected late Eocene glaciation, *Paleoceanography*, 29, 2014PA002648,
16 10.1002/2014PA002648, 2014.

17 Scher, H. D., Whittaker, J. M., Williams, S. E., Latimer, J. C., Kordesch, W. E., and Delaney,
18 M. L.: Onset of Antarctic Circumpolar Current 30 million years ago as Tasmanian Gateway
19 aligned with westerlies, *Nature*, 523, 580-583, 2015.

20 Seton, M., Müller, R., Zahirovic, S., Gaina, C., Torsvik, T., Shephard, G., Talsma, A.,
21 Gurnis, M., Turner, M., and Maus, S.: Global continental and ocean basin reconstructions
22 since 200Ma, *Earth Sci. Rev.*, 113, 212-270, 2012.

23 Sexton, P. F., Wilson, P. A., and Norris, R. D.: Testing the Cenozoic multisite composite
24 $\delta(18)\text{O}$ and $\delta(13)\text{C}$ curves: New monospecific Eocene records from a single locality,
25 Demerara Rise (Ocean Drilling Program Leg 207), *Paleoceanography*, 21, PA2019,
26 doi:10.1029/2005PA001253, 2006.

27 Shackleton, N., and Kennett, J.: Paleotemperature history of the Cenozoic and the initiation
28 of Antarctic glaciation: oxygen and carbon isotope analyses in DSDP Sites 277, 279, and
29 281, in: Kennett, J.P., Houtz, R. E., et al., Initial reports of the deep sea drilling project, Vol.
30 29, 743-755, 1975.

1 [Spencer-Cervato, C.: The Cenozoic deep sea microfossil record: explorations of the](#)
2 [DSDP/ODP sample set using the Neptune database, *Palaeontologia Electronica*, 2, 270, 1999.](#)

3 Spiess, V.: Cenozoic magnetostratigraphy of Leg 113 drill sites, Maud Rise, Weddell Sea,
4 Antarctica, Proceedings ODP, Scientific Results, 113, Ocean Drilling Program, College
5 Station, TX, 261–315, doi:10.2973/odp.proc.sr.113.182.1990, 1990.

6 Stickley, C. E., Brinkhuis, H., Schellenberg, S. A., Sluijs, A., Röhl, U., Fuller, M., Grauert,
7 M., Huber, M., Warnaar, J., and Williams, G. L.: Timing and nature of the deepening of the
8 Tasmanian Gateway, *Paleoceanography*, 19, PA4027, doi:10.1029/2004PA001022, 2004.

9 [Sutherland, R.: The Australia-Pacific boundary and Cenozoic plate motions in the SW](#)
10 [Pacific: Some constraints from Geosat data, *Tectonics*, 14, 819-831, 1995.](#)

11 Suzuki, N., Ogane, K., and Chiba, K.: Middle to Late Eocene polycystine radiolarians from
12 the Site 1172, Leg 189, Southwest Pacific, *News of Osaka Micropaleontologists*, special
13 volume, 14, 239-296, 2009.

14 Takemura, A.: Radiolarian Paleogene biostratigraphy in the southern Indian Ocean, Leg 120,
15 in: Wise, S.W. Jr., Schlich, R. et al., , Proceedings ODP, Scientific Results, 120, Ocean
16 Drilling Program, College Station, TX, 735–756, doi:10.2973.odp.proc.sr.120.177, 1992.

17 Takemura, A., and Ling, H. Y.: Eocene and Oligocene radiolarian biostratigraphy from the
18 Southern Ocean - correlation of ODP Legs 114 (Atlantic Ocean) and 120 (Indian Ocean),
19 *Mar.~~ine~~ Micropaleontol.~~ogy~~*, 30, 97-116, 1997.

20 [Torsvik, T. H., Van der Voo, R., Preeden, U., Mac Niocaill, C., Steinberger, B., Doubrovine,](#)
21 [P. V., van Hinsbergen, D. J., Domeier, M., Gaina, C., and Tohver, E.: Phanerozoic polar](#)
22 [wander, palaeogeography and dynamics, *Ear. Sci. Rev.*, 114, 325-368, 2012.](#)

23 [van Hinsbergen, D. J., de Groot, L. V., van Schaik, S. J., Spakman, W., Bijl, P. K., Sluijs, A.,](#)
24 [Langereis, C. G., and Brinkhuis, H.: A Paleolatitude Calculator for Paleoclimate Studies,](#)
25 [*PloS one*, 10, e0126946, 2015.](#)

26 Villa, G., Fioroni, C., Pea, L., Bohaty, S., and Persico, D.: Middle Eocene–late Oligocene
27 climate variability: calcareous nannofossil response at Kerguelen Plateau, Site 748, *Mar.~~ine~~*
28 *Micropaleontol.~~ogy~~*, 69, 173-192, 2008.

29 Vonhof, H. B., Smit, J., Brinkhuis, H., Montanari, A., and Nederbragt, A. J.: Global cooling
30 accelerated by early late Eocene impacts?, *Geology*, 28, 687-690, 2000.

- 1 Westerhold, T., Röhl, U., Pälike, H., Wilkens, R., Wilson, P., and Acton, G.: Orbitally tuned
2 time scale and astronomical forcing in the middle Eocene to early Oligocene, *Clim. ~~ate of the~~*
3 *Past ~~Discussions~~*, *910*, ~~6635-6682~~*955-973*, [doi:10.5194/cp-10-955-2014](https://doi.org/10.5194/cp-10-955-2014), 2014.
- 4 Zachos, J. C., Quinn, T. M., and Salamy, K. A.: High-resolution (104 years) deep-sea
5 foraminiferal stable isotope records of the Eocene-Oligocene climate transition,
6 *Paleoceanography*, 11, 251-266, 1996.
- 7 Zachos, J. C., Pagani, M., Sloan, L., Thomas, E., and Billups, K.: Trends, rhythms, and
8 aberrations in global climate 65 Ma to present, *Science*, 292, 686-693, 2001.
- 9

Table 1: Summary of species for which biogeographic affinities have been established and their presence (x) encountered at sites 277, 280, 281, and 283, and 1172. their biogeographic affinity (AH=Antarctic-high-latitude (>45°N/S), B=bipolar, L=low-latitude (<25°N/S) and C=cosmopolitan.), and location of photographic images on plates for selected species.

Taxa	Biogeogr. affinity	Site 277	Site 280	Site 281	Site 283	ODP 1172	Plate
<i>Amphicentria</i> sp. 1 sensu Suzuki	H	x		x	x	x	Pl. 2, Fig. 1
<i>Amphicraspedum murrayanum</i> Haeckel	L	x					Pl. 1, Fig. 14
<i>Amphicraspedum prolixum</i> Sanfilippo and Riedel gr.	L	x	x				Pl. 1, Fig. 15-17
<i>Amphisphaera coronata</i> (Ehrenberg) gr.	C	x			x	x	Pl. 1, Fig. 2
<i>Amphisphaera spinulosa</i> (Ehrenberg)	C	x			x		Pl. 1, Fig. 5
<i>Amphymenium splendidiarmatum</i> Clark and Campbell	C	x	x	x	x		Pl. 1, Fig. 18,19
<i>Antarctissa cylindrica</i> Petrushevskaya	H		x				
<i>Antarctissa robusta</i> Petrushevskaya	H		x				
<i>Aphetocyrtis bianulus</i> (O'Connor)	H	x			x	x	Pl. 5, Fig. 1
<i>Aphetocyrtis gnomabax</i> Sanfilippo and Caulet	H	x	x	x	x		Pl. 5, Fig. 2-7
<i>Aphetocyrtis rossi</i> Sanfilippo and Caulet	H	x	x		x		Pl. 5, Fig. 8-11
<i>Artobotrrys auriculaleporis</i> (Clark and Campbell)	C	x				x	
<i>Artostrobos annulatus</i> (Bailey)	H	x			x		
<i>Artostrobos</i> cf. <i>pretubulatus</i> Petrushevskaya	H	x					Pl. 3, Fig. 13
<i>Aspis</i> sp. A sensu Hollis	H	x	x		x		Pl. 3, Fig. 14-16
<i>Axoprunum bispiculum</i> (Popofsky)	H	x			x		
<i>Axoprunum pierinae</i> (Clark and Campbell) gr.	C	x	x	x	x	x	Pl. 1, Fig. 10,11
<i>Axoprunum?</i> <i>irregularis</i> Takemura	H	x				x	Pl. 1, Fig. 12
<i>Ceratocyrtis</i> spp.	H	x	x		x	x	Pl. 2, Fig. 3-5
<i>Cinctopyramis circumtexta</i> (Haeckel)	C	x	x	x	x	x	
<i>Clathrocyclus universa</i> Clark and Campbell	C	x		x	x	x	
<i>Clinorhabdus anantomus</i> Sanfilippo and Caulet	H	x		x	x		Pl. 5, Fig. 12,13
<i>Clinorhabdus robusta</i> (Abelmann)	H					x	
<i>Comutella profunda</i> Ehrenberg	C	x	x	x	x	x	
<i>Cryptocarpium bussonii</i> (Carnevale) gr.	C	x	x	x	x	x	Pl. 5, Fig. 25a,b, 26a,b
<i>Cryptocarpium ornatum</i> (Ehrenberg)	C	x			x		
<i>Cycladophora cosma cosma</i> Lombardi and Lazarus	H		x				Pl. 3, Fig. 17
<i>Cycladophora humerus</i> (Petrushevskaya)	H		x	x	x		Pl. 3, Fig. 18
<i>Cycladophora</i> spp.	H	x		x	x		
<i>Cyrtolagena laguncula</i> Haeckel	C	x			x		
<i>Dictyophimus pocillum</i> Ehrenberg	C	x					
<i>Dictyophimus?</i> aff. <i>archipilium</i> Petrushevskaya	H	x		x	x		Pl. 4, Fig. 3a,b-8
<i>Dictyophimus?</i> <i>archipilium</i> Petrushevskaya	H	x	x		x		Pl. 4, Fig. 1a,b, 2
<i>Eucyrtidium antiquum</i> Caulet	H	x	x			x	Pl. 3, Fig. 19
<i>Eucyrtidium mariae</i> Caulet	H	x					
<i>Eucyrtidium nishimurae</i> Takemura and Ling	H			x	x	x	Pl. 3, Fig. 20a, b
<i>Eucyrtidium spinosum</i> Takemura	H	x		x	x	x	Pl. 3, Fig. 21
<i>Eucyrtidium montiparum</i> Ehrenberg	C	x			x		Pl. 3, Fig. 22
<i>Eurystomoskevos cauleti</i> O'Connor	H	x	x	x	x		Pl. 3, Fig. 23a, b
<i>Eurystomoskevos petrushevskae</i> Caulet	H	x	x	x	x	x	Pl. 3, Fig. 24
<i>Eusyringium fistuligerum</i> (Ehrenberg)	C	x				x	Pl. 3, Fig. 25
<i>Eusyringium lagena</i> (Ehrenberg)	C				x		
<i>Glycobotrrys nasuta</i> (Ehrenberg) gr.	C	x	x	x	x	x	Pl. 3, Fig. 5-7
<i>Lamprocyclus particolis</i> O'Connor	H	x	x	x	x		Pl. 5, Fig. 27
<i>Larcopele</i> cf. <i>pylomaticus</i> (Riedel)	H		x	x			Pl. 1, Fig. 25a, b
<i>Larcopele frakesi</i> (Chen)	H		x				Pl. 1, Fig. 20
<i>Larcopele hayesi</i> (Chen)	H	x	x	x	x		Pl. 1, Fig. 21
<i>Larcopele labyrinthosa</i> Lazarus	H		x				Pl. 1, Fig. 22
<i>Larcopele polyacantha</i> (Campbell and Clark) gr.	H	x	x	x	x		Pl. 1, Fig. 23, 24
<i>Larcopele</i> spp.	H	x	x	x			
<i>Lithelius minor</i> Jørgensen gr.	C	x	x	x	x	x	Pl. 1, Fig. 26-28
<i>Lithomelissa challengerae</i> Chen	H		x				Pl. 2, Fig. 6-8
<i>Lithomelissa ehrenbergi</i> Bütschli	H	x	x	x	x	x	Pl. 2, Fig. 10, 11

<i>Lithomelissa gelatinus</i> O'Connor	H	x	x	x	x		Pl. 2, Fig. 12, 13
<i>Lithomelissa robusta</i> Chen	H		x		x		Pl. 2, Fig. 16
<i>Lithomelissa sphaerocephalis</i> Chen	H	x	x	x	x		Pl. 2, Fig. 17
<i>Lithomelissa</i> spp.	H	x	x	x	x		
<i>Lithomelissa tricornis</i>	H	x	x	x	x		Pl. 2, Fig. 18
<i>Lithomelissa?</i> <i>sakaii</i> O'Connor	H		x				Pl. 2, Fig. 19
<i>Lophocyrtis</i> (<i>Apoplanius</i>) <i>aspera</i> (Ehrenberg)	H	x		x	x		Pl. 5, Fig. 14a, b-16
<i>Lophocyrtis</i> (<i>Apoplanius</i>) <i>keraspera</i> Sanfilippo and Caulet	H	x			x	x	Pl. 5, Fig. 17-19
<i>Lophocyrtis</i> (<i>Lophocyrtis</i>) <i>jacchia hapsis</i> Sanfilippo and Caulet	H	x			x		Pl. 5, Fig. 20-22
<i>Lophocyrtis</i> (<i>Paralampterium</i>) <i>dumitricai</i> Sanfilippo	C	x				x	
<i>Lophocyrtis</i> (<i>Paralampterium</i>) <i>longiventer</i> (Chen)	H	x	x	x	x	x	Pl. 5, Fig. 23, 24
<i>Lophocyrtis</i> spp.	H				x		
<i>Lophphaena capito</i> Ehrenberg	C	x		x	x		
<i>Lychnocanium amphirrite</i> (Foreman)	C	x			x	x	Pl. 4, Fig. 11a, b, c, 12
<i>Lychnocanium babylonis</i> (Clark and Campbell)	C	x			x		Pl. 4, Fig. 13a, b, 14
<i>Lychnocanium bellum</i> Clark and Campbell	C	x			x	x	Pl. 4, Fig. 15, 16
<i>Periphaena decora</i> Ehrenberg	C	x	x	x	x	x	
<i>Periphaena heliastericus</i> (Clark and Campbell)	C	x	x	x	x	x	
<i>Plectodiscus circularis</i> (Clark and Campbell)	C	x	x	x	x	x	
<i>Pseudodictyophimus galeatus</i> Caulet	H		x				Pl. 2, Fig. 20
<i>Pseudodictyophimus gracilipes</i> (Bailey) gr.	H	x	x	x	x		Pl. 2, Fig. 21-23
<i>Pseudodictyophimus</i> spp.	H		x				Pl. 2, Fig. 24-27
<i>Sethocyrtis chrysallis</i> Sanfilippo and Blome	C	x					Pl. 3, Fig. 26a, b
<i>Siphocampe nodosaria</i> (Haeckel)	C	x		x	x	x	
<i>Siphocampe quadrata</i> (Petrushevskaya and Kozlova)	C	x		x	x	x	
<i>Siphocampe?</i> <i>amygdala</i> (Shilov)	C	x			x		Pl. 3, Fig. 11, 12
<i>Sphaeropyle tetrapila</i> (Hays)	H	x					Pl. 1, Fig. 29
<i>Spirocyrtes joides</i> (Petrushevskaya)	C	x	x	x	x		
<i>Spongodiscus cruciferus</i> (Clark and Campbell)	C	x		x		x	
<i>Spongodiscus festinus</i> (Clark and Campbell)	C	x				x	
<i>Spongopyle osculosa</i> Dreyer	H	x	x	x	x	x	Pl. 1, Fig. 13
<i>Spongurus bilobatus</i> Clark and Campbell	C	x		x	x	x	
<i>Stylosphaera minor</i> Clark and Campbell gr.	C	x	x		x	x	Pl. 1, Fig. 7
<i>Theocampe amphora</i> (Haeckel)	C	x					
<i>Theocampe urceolus</i> (Haeckel)	C	x	x	x	x		
<i>Theocyrtis tuberosa</i> Riedel	L	x			x		Pl. 5, Fig. 30
<i>Thyrsoyrtis pinguicoides</i> O'Connor	L	x			x		Pl. 3, Fig. 27
<i>Tripodiscinus clavipes</i> (Clark and Campbell)	C	x		x	x		
<i>Zealithapium mitra</i> (Ehrenberg)	C	x			x		Pl. 1, Fig. 8

1

2

Table 2: Average of total % of high-latitude species, groups, genera and high-latitude members of families for ~~four~~ five time slices: Middle Eocene Climatic Optimum (MECO₂ (~40–40 Ma), early late Eocene/PrOM (~38–37 Ma), late Eocene warming event (~36 Ma), latest Eocene-earliest Oligocene (~35–32 Ma)middle/late Eocene (~39–38 Ma), late Eocene (~37–35 Ma) and early Oligocene (~33–30 Ma).

	Site 277					Site 280	Site 281	Site 283	Site 1172			
	40 Ma	38–37 Ma	36 Ma	35–32 Ma	30 Ma	e. Olig.	38–37 Ma	38–37 Ma	36 Ma	40 Ma	l Eoc	e Olig.
% high-latitude species	23.2	28.9	13.7	39.0	100.0	62.6	61.2	28.0	25.6	7.8	26.8	66.1
<i>Larcopyle</i> spp. %	6.9	2.9	2.5	6.2	-	18.4	26.5	3.0	1.8	-	-	7.0
<i>Lithomelissa</i> spp. %	0.1	1.8	0.1	5.9	-	16.4	11.8	4.1	4.8	0.4	0.7	0.8
High-lat. Lophocyrtidae %	14.9	20.8	8.0	16.7	3.3	10.4	14.2	8.5	6.9	4.1	19.3	5.7
High-lat. Eucyrtidae %	-	0.4	0.5	1.8		8.8	6.3	7.4	9.1	3.3	5.3	-
Other high-lat. Plagiacanthidae %	-	0.2	-	1.4		6.5	1.4	1.8	1.5	-	-	0.2
Other high-lat. species %	1.3	2.8	2.7	7.0	96.7	2.0	1.1	3.1	1.5	0.1	1.6	52.5
% cosmopolitan species	72.6	71.1	80.9	59.9	-	37.3	38.8	71.8	65.2	92.2	73.2	33.9
% low-latitude species	4.2	0.1	5.4	1.0	-	0.1	-	0.1	9.2	-	-	-

1 Figures

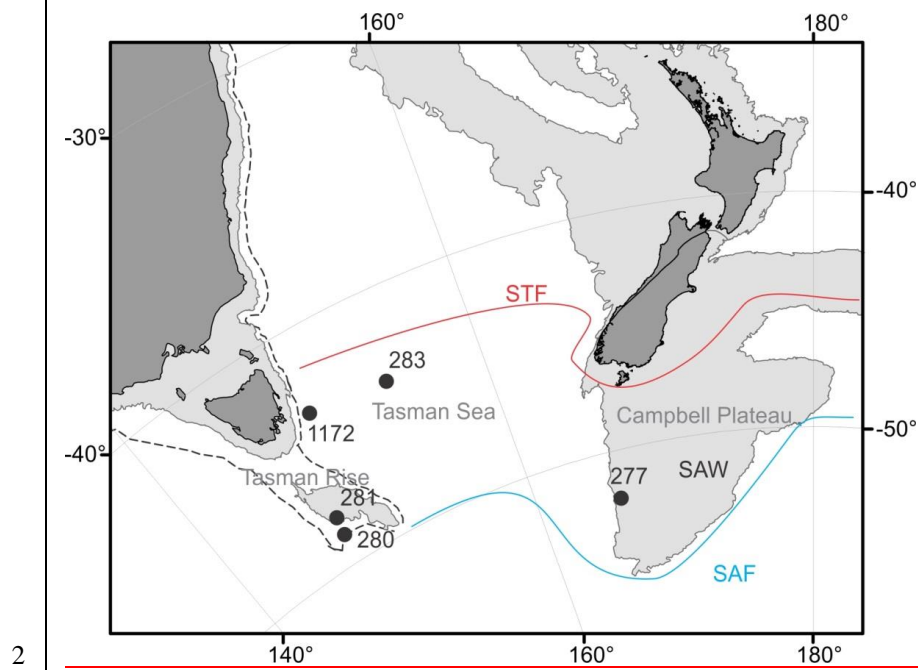


Figure 1. Modern location of DSDP and ODP study sites in the Southwest Pacific; dark grey=coastline, light grey=2000 m isobath of continental boundary. STF=Subtropical Front, SAF=Subantarctic Front, SAW=Subantarctic Water.

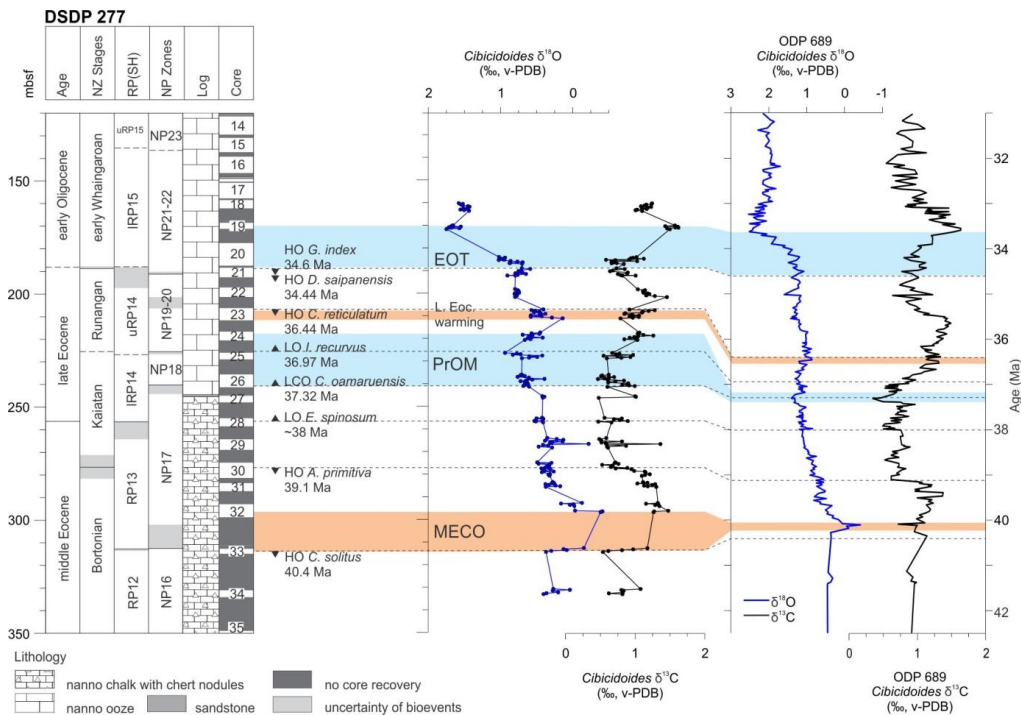


Figure 2. DSDP Site 277 stratigraphy, NZ Stages (Raine et al. (2015), Southern Ocean Hemisphere radiolarian zones (RP), nannofossil zones (NP), lithology, core recovery, selected bioevents (ages calibrated to the 2012 geological timescale; Gradstein et al., 2012; Raine et al., 2015) ranges of *Globigerinatheka index* and selected radiolarians and Benthic $\delta^{18}\text{O}$ stable oxygen and $\delta^{13}\text{C}$ carbon isotope data of DSDP Site 277. The dashed lines correlate Site 277 based on the ages of the bioevents to correlated to Southern Ocean *Cibicidoides* data of ODP Site 689 Hole B (Maud Rise) (Diester-Haass and Zahn, 1996) calibrated to the GTS2012 timescale using the magnetostratigraphy data of Florindo and Roberts (2005) and Spiess (1990). LO=Lowest Occurrence; LCO=Lowest Common Occurrence; HO=Highest Occurrence; MECO=Middle Eocene Climatic Optimum; PrOM=Priabonian Oxygen Isotope Maximum; EOT=Eocene-Oligocene transition.

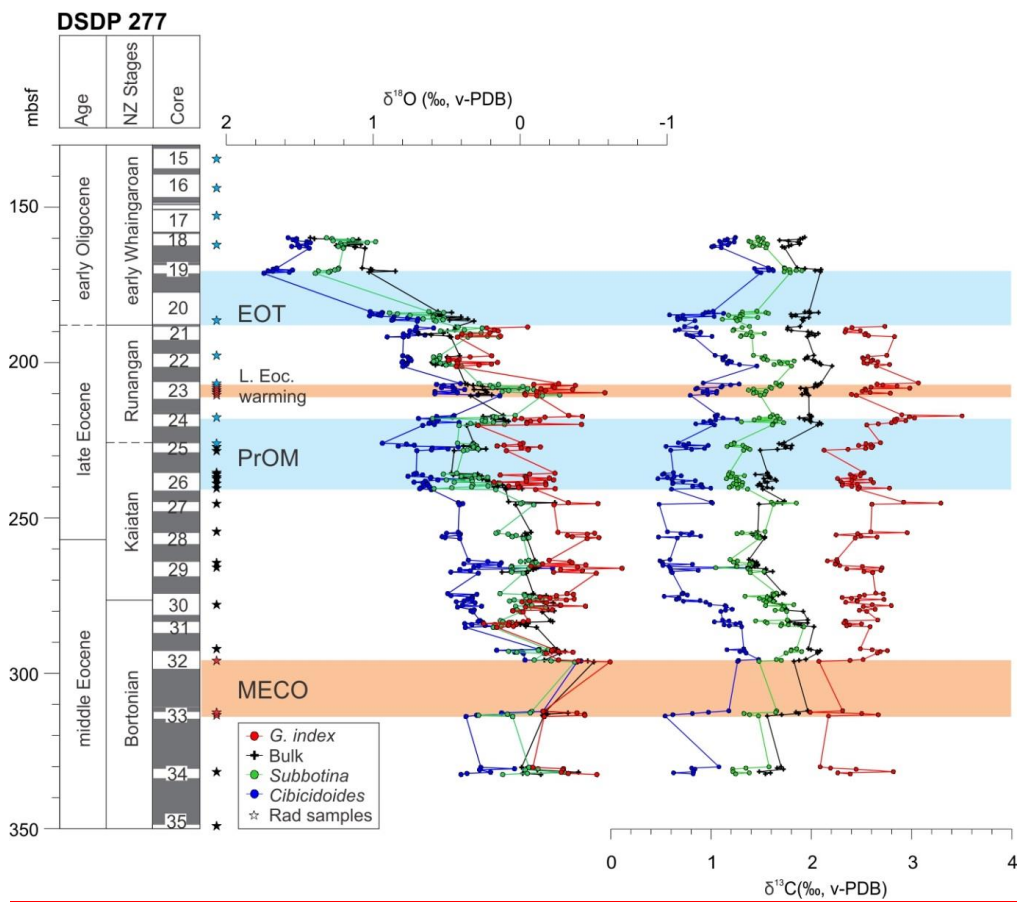


Figure 3. DSDP Site 277 $\delta^{18}\text{O}$ and $\delta^{13}\text{C}$ oxygen and carbon stable isotope records and position-location of studied radiolarian samples within the MECO and late Eocene warming interval (red stars) and radiolarian-rich late-upper Eocene-lower Oligocene interval (blue stars).

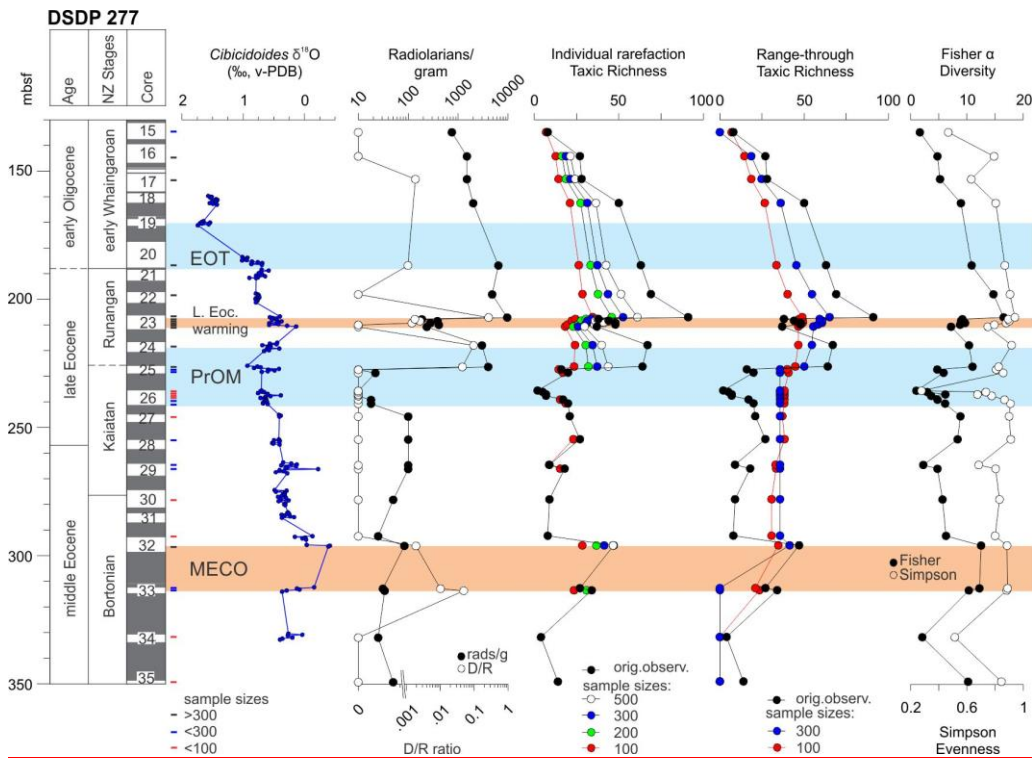


Figure 4. DSDP Site 277 benthic $\delta^{18}\text{O}$ record; radiolarian abundance and Diatom/Radiolarian (D/R) ratio; Taxic Richness (number of taxa) derived from individual rarefaction and range-through analyses for different sample sizes; Fisher α Index and Simpson Evenness Index for radiolarian assemblages. Red bars indicate sample sizes <100 specimens, blue bars for samples sizes <300 specimens and black bars for samples >300 specimens. Red arrows indicate samples with total specimen counts less than 99, which may be statistical insignificant but are included in all figures for the sake of completeness.

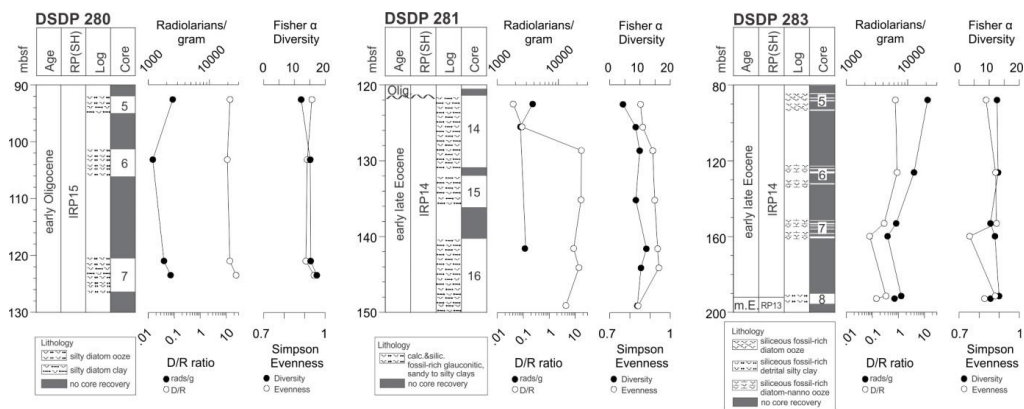


Figure 5. Stratigraphy, Southern Hemisphere radiolarian zones (RP), lithology and core recovery at DSDP sites 280, 281 and 283. Variation in radiolarian abundance, Diatom/Radiolarian (D/R) ratio, Fisher α Index and Simpson Evenness for radiolarian assemblages at DSDP sites 280, 281 and 283 all sites.

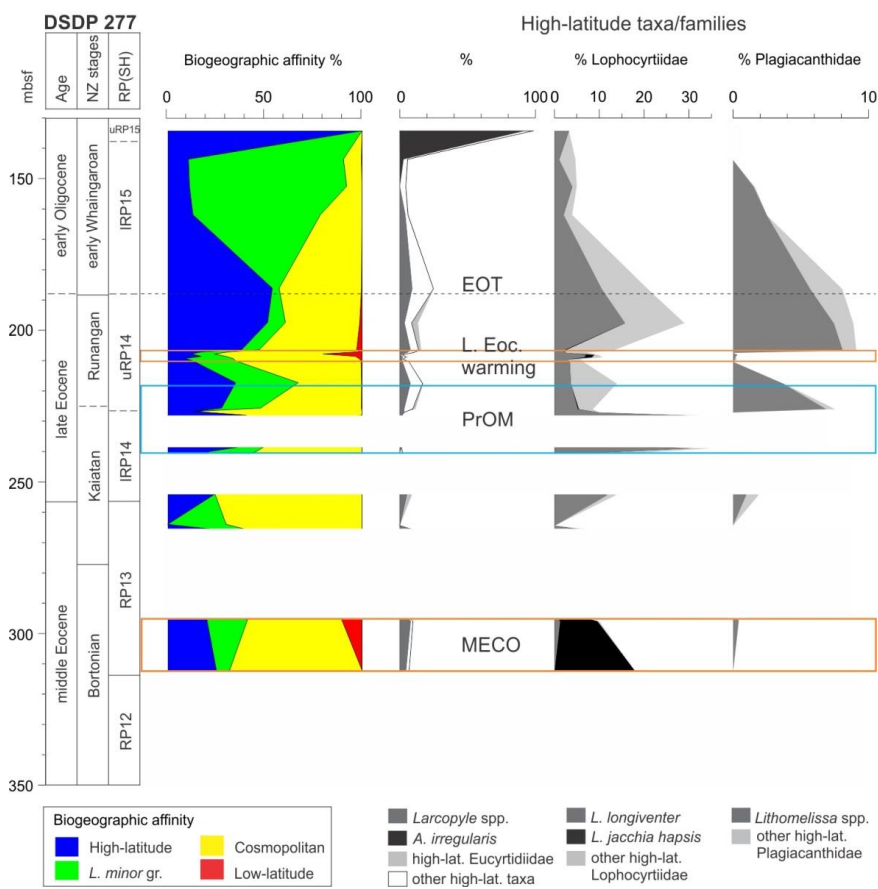


Figure 6. Biogeographic affinities of radiolarian assemblages at DSDP Site 277 and the abundance of high-latitude taxa/families.; ~~Taxic richness; most abundant families with high-latitude affinity. Red arrows indicate samples with total specimen counts less than 99.~~ MECO=Middle Eocene Climatic Optimum, PrOM=Priabonian Oxygen Isotope Maximum, EOT=Eocene-Oligocene transition.

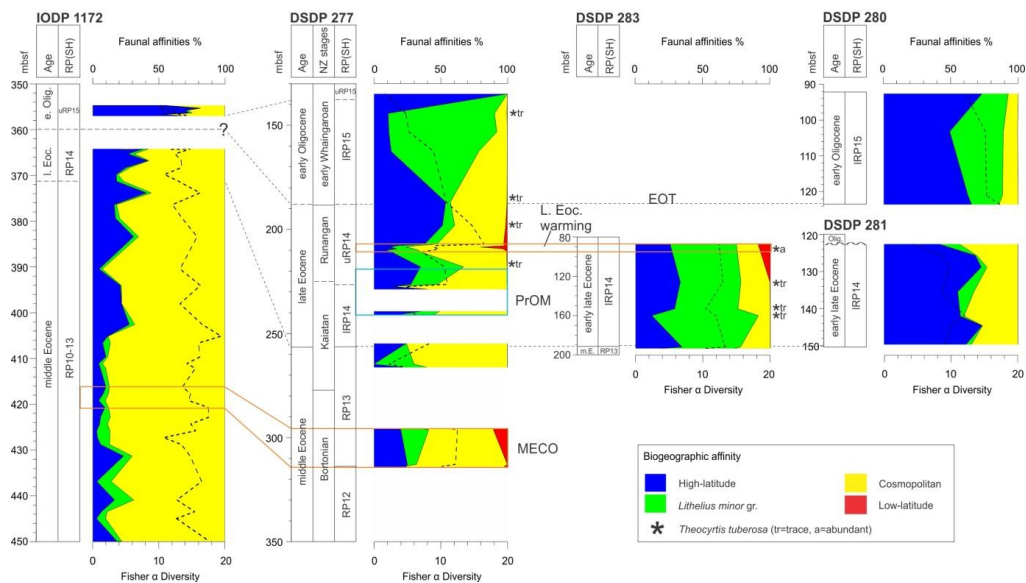


Figure 7. Variation in faunal affinities for radiolarians assemblages and Fisher α Diversity at all sites. Dashed black lines indicate correlation between sites, which is hampered by hiatuses and poorly defined ages, respectively. The location of the MECO at Site 1172 is taken from Bijl et al. (2010). The age model of ODP Site 1172 is based on the age-depth plot of Stickley et al. (2004).

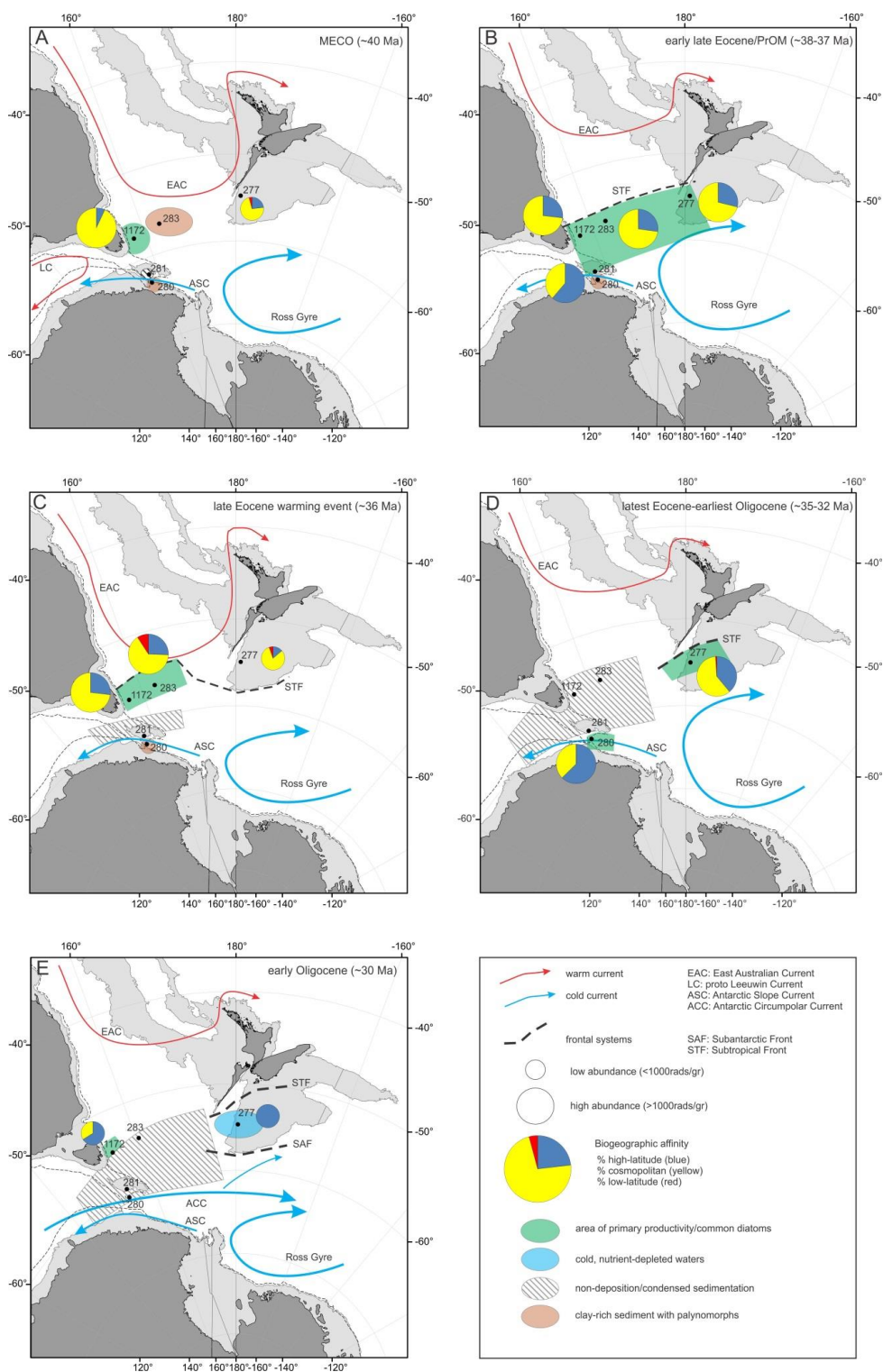


Figure 8. Paleogeographic reconstructions and biogeographic affinities at investigated sites during the MECO (~40 Ma), early late Eocene/PrOM (~38–37 Ma), late Eocene warming event (~36 Ma), latest Eocene-earliest Oligocene (~35–32 Ma), and early Oligocene (~30 Ma). The 2000 m isobath from the GEBCO (www.gebco.net) bathymetric grid was used to approximate continental boundaries (light grey). The continental/oceanic boundaries of Bird (2003) are also shown for reference (dashed lines); continents with present day shorelines are in dark grey. The late Eocene average is plotted for Site 1172 in map B and C.

~~Paleogeographic reconstructions (GPlates, using the latest hotspot trace reference frames (Seton et al., 2012; Matthews et al., 2015)) and biogeographic affinities at investigated sites during the MECO, middle/late Eocene (~39–38 Ma), PrOM and latest Eocene (~37–35 Ma) and early Oligocene (~33 Ma).~~